doi:10.1093/plcell/koaa007

THE PLANT CELL

THE PLANT CELL 2021: 33: 153–171

Research Article

EDS1-interacting J protein 1 is an essential negative regulator of plant innate immunity in Arabidopsis

Hailun Liu [1,†] Yuge Li [1,†] Yilong Hu [1] Yuhua Yang [1] Wenbin Zhang [1,2] Ming He [1,2] Xiaoming Li [1] Chunyu Zhang [1] Fanjiang Kong [3] Xu Liu [1,4] and Xingliang Hou [1,4,*]

1 Key Laboratory of South China Agricultural Plant Molecular Analysis and Genetic Improvement & Guangdong Provincial Key Laboratory of Applied Botany, South China Botanical Garden, Chinese Academy of Sciences, Guangzhou, China
2 University of Chinese Academy of Sciences, Beijing, China
3 School of Life Sciences, Guangzhou University, Guangzhou 510006, China
4 Center of Economic Botany, Core Botanical Gardens, Chinese Academy of Sciences, Guangzhou, China

*Author for communication: houxl@scib.ac.cn
†These authors contributed equally to this work.

H.L. and X.H. designed research; H.L., Y.L., Y.H., Y.Y., W.Z., and M.H. performed the research; H.L., Y.H., M.H., C.Z., F.K., X.L., and X.H. analyzed data; H.L. and X.H. wrote the article. The authors declare no competing interests.
The author responsible for distribution of materials integral to the findings presented in this article in accordance with the policy described in the Instructions for Authors (www.plantcell.org) is: Xingliang Hou (houxl@scib.ac.cn)

Abstract

Plants have evolved precise mechanisms to optimize immune responses against pathogens. ENHANCED DISEASE SUSCEPTIBILITY 1 (EDS1) plays a vital role in plant innate immunity by regulating basal resistance and effector-triggered immunity. Nucleocytoplasmic trafficking of EDS1 is required for resistance reinforcement, but the molecular mechanism remains elusive. Here, we show that EDS1-INTERACTING J PROTEIN1 (EIJ1), which acts as a DnaJ protein-like chaperone in response to pathogen infection, functions as an essential negative regulator of plant immunity by interacting with EDS1. The loss-of-function mutation of *EIJ1* did not affect plant growth but significantly enhanced pathogen resistance. Upon pathogen infection, EIJ1 relocalized from the chloroplast to the cytoplasm, where it interacted with EDS1, thereby restricting pathogen-triggered trafficking of EDS1 to the nucleus and compromising resistance at an early infection stage. During disease development, EIJ1 was gradually degraded, allowing the nuclear accumulation of EDS1 for transcriptional resistance reinforcement. The avirulent strain *Pst* DC3000 (AvrRps4) abolished the repressive action of EIJ1 by rapidly inducing its degradation in the effector-triggered immunity response. Thus, our findings show that EIJ1 is an essential EDS1-dependent negative regulator of innate plant immunity and provide a mechanistic understanding of how the nuclear versus cytoplasmic distribution of EDS1 is regulated during the immune response.

Introduction

Plants have evolved a complicated network to modulate their immune responses. To defend themselves against pathogens, plants employ two main regulatory strategies: pattern-triggered immunity (PTI), and effector-triggered immunity (ETI). PTI is governed by pattern recognition receptors (PRRs) that recognize pathogen- or microbe-associated molecular patterns (Zipfel, 2008). To facilitate infection, virulent pathogens suppress PTI by secreting pathogen effectors, and they manipulate host cells to facilitate nutrient acquisition and ultimately reproduction (Tsuda and Katagiri, 2010). The low-level resistance that the plant

Received February 3, 2020. Accepted October 23, 2020. Advance access publication November 23, 2020

IN A NUTSHELL

Background: Plants have evolved a complicated network to modulate the immune response. To defend themselves against pathogens, plants employ two main regulatory strategies: pattern-triggered immunity (PTI) and effector-triggered immunity (ETI). PTI is governed by pattern recognition receptors. To facilitate infection, virulent pathogens suppress PTI by secreting pathogen effectors. The low-level resistance that the plant displays to these virulent pathogens is termed as basal resistance. On the other hand, ETI is mediated by plant-encoded disease resistance (R) proteins, which can directly or indirectly recognize the presence of effectors secreted by pathogens. Compared with basal resistance, ETI induces a stronger and faster defense response against pathogens and is often accompanied by local cell death, a characteristic feature of the hypersensitive response.

Questions: Does EIJ1 function as a negative regulator of plant innate immunity and what is the molecular mechanism?

Findings: We found that EIJ1, which acts as a chaperone DnaJ protein in response to pathogen infection, functions as an essential negative regulator of plant immunity by interacting with EDS1. The loss-of-function mutation of EIJ1 did not affect plant growth but significantly enhanced pathogen resistance. Upon pathogen infection, EIJ1 relocalized from the chloroplast to cytoplasm, where it interacted with EDS1, thereby restricting the pathogen-triggered trafficking of EDS1 to the nucleus and compromising resistance at an early infection stage. Over the course of disease development, EIJ1 was gradually degraded, allowing the nuclear accumulation of EDS1 for transcriptional resistance reinforcement.

Next steps: Normally, EIJ1 is located in the chloroplast. When the plants are invaded by pathogens, the EIJ1 protein will be rapidly released to the cytoplasm. Next, our studies will focus on whether the effectors in Pst DC3000 promote the transfer of EIJ1 from chloroplasts to the cytoplasm.

displays to these virulent pathogens is termed as basal resistance (Jones and Dangl, 2006; Klessig et al., 2018). On the other hand, ETI is mediated by plant-encoded disease resistance (R) proteins, which can directly or indirectly recognize the presence of effectors secreted by pathogens (Tsuda and Katagiri, 2010). Most R proteins contain a nucleotide-binding site and a leucine-rich repeat domain (NB-LRR). The NB-LRR proteins that contain an N-terminal Toll/Interleukin-1 receptor (TIR) protein–protein interaction domain are known as TIR-NB-LRR (TNL) proteins, and they comprise the largest group of NB-LRR proteins (Caplan et al., 2008). Compared with basal resistance, ETI induces a stronger and faster defense response against pathogens and is often accompanied by local cell death, a characteristic feature of the hypersensitive response (HR; Dodds and Rathjen, 2010).

ENHANCED DISEASE SUSCEPTIBILITY 1 (EDS1), a central regulator of plant immunity, helps to control basal resistance by restricting the invasion of biotrophic and hemibiotrophic pathogens (Wiermer et al., 2005). EDS1 also plays an important role in ETI, which is mainly mediated by the TNL class of R proteins (Heidrich et al., 2012). EDS1 works closely with its coregulators PHYTOALEXIN DEFICIENT 4 and SENESCENCE-ASSOCIATED GENE 101 in the cytoplasm and/or nucleus to regulate intracellular reactive oxygen species (ROS) production, salicylic acid (SA) accumulation, and other processes, thus reinforcing pathogen resistance (Rustérucci et al., 2001; Rietz et al., 2011; Wagner et al., 2013). Accordingly, the Arabidopsis *eds1* mutant is highly susceptible to *Pseudomonas syringae* pv. *tomato* (*Pst*) strain DC3000 and shows a compromised TNL-mediated ETI, in which *ISOCHORISMATE SYNTHASE1* (*ICS1*; a SA biosynthetic gene) expression and SA biosynthesis are inhibited (Parker et al., 1996; Feys et al., 2001; Bartsch et al., 2006). Additionally, EDS1 exhibits protein trafficking between the cytoplasm and nucleus mediated by nuclear transport receptors (García et al., 2010). Although the nuclear functions of EDS1 involve basal resistance and ROS production, programmed cell death and resistance reinforcement require coordination of the nuclear versus cytoplasmic localization of EDS1 (Heidrich et al., 2011). A balance between the amount of EDS1 in the cytosol and the amount in the nucleus is important for efficient basal resistance and TNL-triggered immunity (García et al., 2010). However, how EDS1 maintains the nucleocytoplasmic distribution pattern during plant innate immune responses remains unclear.

DnaJ proteins (or J proteins) are chaperone proteins (Pulido and Leister, 2018) that belong to the cysteine (Cys)-rich domain superfamily and participate in the folding and assembly of nascent proteins, transport of proteins across membranes with subsequent refolding, and disposal of unfolded or defective proteins (Bukau et al., 2006). These processes are required for the normal function of most cellular proteins at different developmental stages (Pulido and Leister, 2018). Research in various organisms shows that DnaJ proteins also play diverse roles in biotic and abiotic stress responses, especially in immune responses. In *Nicotiana benthamiana*, DnaJ protein Nb-MIP1 functions as a cochaperone in the response to viral pathogens (Du et al., 2013). Soybean (*Glycine max* L.) Gm-heat shock protein 40 (HSP40.1), a nucleus-localized DnaJ protein, is a positive regulator of resistance to soybean mosaic virus (Liu and Whitham, 2013). In tomato (*Solanum lycopersicum*), the chloroplast-localized DnaJ protein, Le-CDJ2, was reported to improve resistance to the bacterial pathogen, *Pseudomonas solanacearum* (Wang et al., 2014). In addition, Tsi1-interacting protein1 (Tsip1), a tobacco (*Nicotiana tabacum*)

DnaJ protein, was reported to regulate Tsi1-mediated transcriptional activation in response to stress (Ham et al., 2006). These results indicate clearly that DnaJ proteins play an important role in plant immunity, although the underlying mechanisms require further investigation.

In this study, we isolated *Arabidopsis thaliana* EDS1 INTERACTING J PROTEIN 1 (EIJ1), a HSP40-like DnaJ protein, and showed that EIJ1 interacted with EDS1 in planta. The loss-of-function *eij1* mutant plants showed normal growth, stronger pathogen resistance, and higher expression of resistance-related genes upon infection by pathogens compared with wild-type plants. However, the loss-of-function mutation of *EIJ1* did not rescue the susceptible phenotype of the *eds1* mutant upon challenge with *Pst* DC3000. Furthermore, the EIJ1 protein, which normally localizes to the chloroplast, was released from the chloroplast to the cytoplasm upon pathogen inoculation, where it interacted with EDS1, thus preventing its pathogen-triggered trafficking to the nucleus and consequently compromising the resistance response at an early infection stage. These findings elucidate important details of the regulatory mechanism underlying the nucleocytoplasmic distribution pattern of EDS1, and provide a potential effective target for disease resistance breeding in crops.

Results

EIJ1 interacts with EDS1 in vitro and in vivo

As an essential component of plant defense responses, EDS1 is located at a key node of the plant innate immunity signaling network. To identify potential interacting protein partners of EDS1, we performed a yeast two-hybrid screening. EDS1 showed strong interaction with an Arabidopsis HSP40-like chaperone protein (AT2G24860) with an unknown function (Figure 1, A and B), belonging to the DnaJ superfamily (Supplemental Figure 1A); this protein is hereafter referred to as EIJ1. Sequence analysis demonstrated that EIJ1 contains 144 amino acid residues, including four Cys-rich Zn finger motifs (CXXCXGXG; Supplemental Figure 1A). Although other angiosperm species have homologs of EIJ1, the closest homologs appear to be limited to Brassicaceae (Supplemental Figure 1B and File S1). Notably, EIJ1 showed sequence similarity with the *N. tabacum* Tsip1 protein, which is involved in pathogen resistance (Supplemental Figure 1B; Ham et al., 2006).

To identify the functional domains responsible for the interaction between EDS1 and EIJ1, two truncated versions of these proteins were used in yeast two-hybrid assays (Figure 1A; Supplemental Figure 1A). The N terminus of EIJ1 showed strong interaction with the full-length EDS1 as well as the EDS1 N terminus but a weak interaction with the EDS1 C terminus (Figure 1B). This suggests that the N terminus of EDS1, containing a lipase-like domain, and the N terminus of EIJ1 are necessary and sufficient for their interaction. Although the C terminus of EIJ1 contains a conserved Cys-rich Zn finger domain that may facilitate its binding to DNA or other proteins, it does not contribute to the interaction with EDS1. Pull-down assays further verified the interaction between EDS1 and EIJ1 in vitro (Figure 1C), while co-immunoprecipitation (Co-IP) assays using $35S_{pro}$:*EIJ1-6HA* $35S_{pro}$:*EDS1-3FLAG* transgenic plants confirmed their interaction in planta (Figure 1D). Taken together, these results demonstrate that EDS1 interacts with EIJ1 both in vitro and in vivo.

Characterization of EIJ1

To determine the subcellular localization of EIJ1, we fused the *EIJ1* open reading frame with the *mCherry* reporter gene under the control of the cauliflower mosaic virus 35S promoter to generate the $35S_{pro}$:*EIJ1-mCherry* construct. This construct was transiently transformed into *N. benthamiana* leaves by agroinfiltration. Fluorescence microscopy showed that EIJ1-mCherry was localized to both the chloroplast and nucleus (Figure 2A). This localization pattern was confirmed by immunoblot analysis of transgenic $35S_{pro}$:*EIJ1-6HA* plants (Supplemental Figure 2). To investigate the expression pattern of *EIJ1*, the genomic sequence of *EIJ1* was fused with the *ß-glucuronidase* (*GUS*) reporter gene to generate $EIJ1_{pro}$:*EIJ1-GUS* transgenic Arabidopsis lines. Strong GUS activity was detected in rosette leaves and roots; however, the GUS activity was weak in siliques and undetectable in stems and flowers (Figure 2B). These results were consistent with the expression results for *EIJ1*, which was examined by quantitative Reverse Transcription-PCR (RT-PCR) in various tissues (Figure 2C).

Given that EDS1 is a central regulator of plant immunity (Saikat et al., 2011), we investigated whether EIJ1, a putative cofactor of EDS1, also is engaged in the response to pathogen infection. The transcript level of *EIJ1* was induced by treatment with either hemibiotrophic bacteria *Pst* DC3000 or SA (Figure 2D). GUS staining revealed that *EIJ1* was induced and markedly concentrated around the trichomes in *Pst* DC3000-inoculated leaves (Figure 2E–G), implying a possible biological relevance of EIJ1 in defense response (Xin and He, 2013). Next, we examined the level of EIJ1 in $35S_{pro}$:*EIJ1-HA* plants treated with *Pst* DC3000 or SA. Interestingly, upon *Pst* DC3000 or SA treatment, EIJ1 was gradually degraded after a quick induction (Figure 2, H and I). This result was not consistent with the stable expression pattern of *EIJ1-HA* observed in $35S_{pro}$:*EIJ1-HA* plants during pathogen infection (Supplemental Figure 3), indicating post-transcriptional regulation of EIJ1. Together, these results suggest that EIJ1 is involved in the plant immune response.

A loss-of-function mutation of *EIJ1* enhances resistance to *Pst* DC3000 via the SA pathway

To investigate the role of EIJ1 in plant immunity, we identified an Arabidopsis mutant (SALK_142975) containing a T-DNA insertion in the third exon of *EIJ1* (Figure 3, A and B). Quantitative RT-PCR analysis showed that *EIJ1* was poorly expressed in this *eij1* T-DNA insertion mutant; therefore, we named this *EIJ1* allele *eij1-1* (Figure 3C). Subsequently, we evaluated the disease resistance phenotype of 3-week-old *eij1-1* mutant plants and Arabidopsis

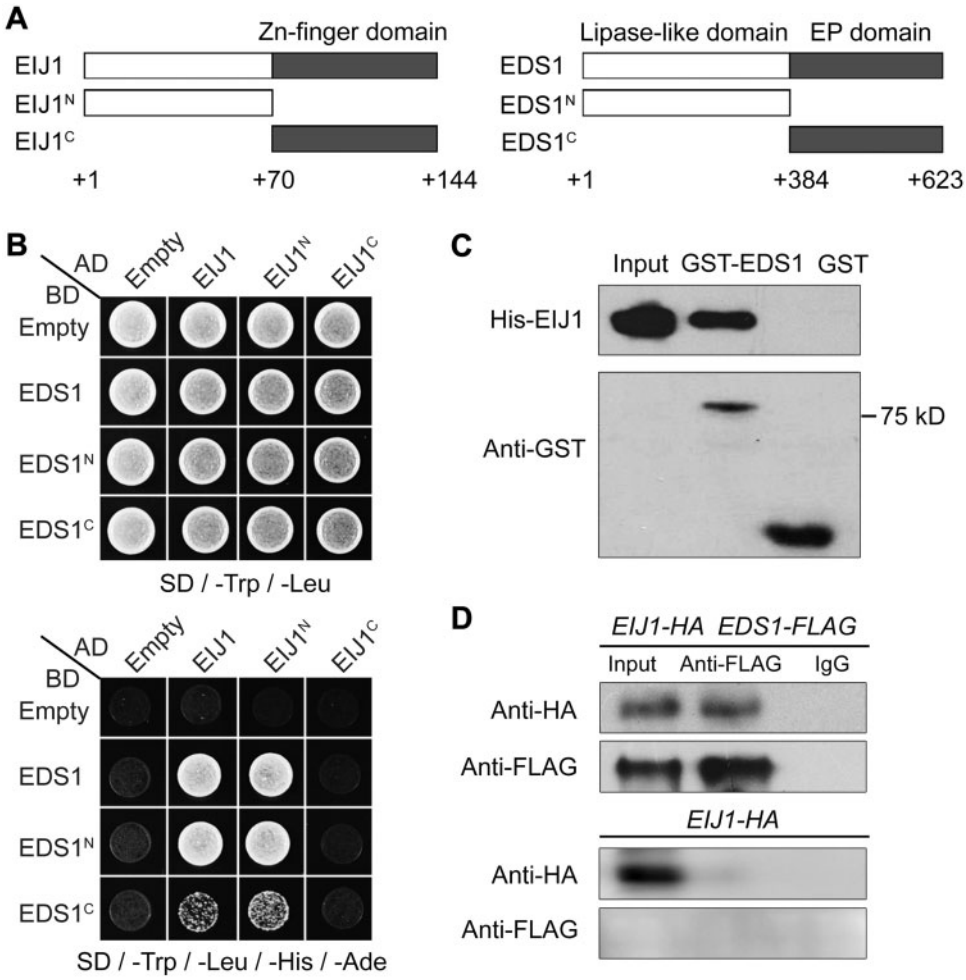

Figure 1 EIJ1 interacts with EDS1 in vitro and in planta. (A) Schematic diagram showing the domains found in EIJ1, EDS1, and their truncated versions. (B) Yeast two-hybrid assays showing the interactions between EIJ1, EDS1, and their truncated versions. Transformed yeast cells were grown on SD/-Trp/-Leu/-His/-Ade and SD/-Trp/-Leu medium. Empty, vector-only controls; AD, activation domain; BD, DNA-binding domain. (C) Pull-down assay showing the direct interaction between His-EIJ1 and GST-EDS1 fusion proteins in vitro. His-EIJ1 proteins were incubated with immobilized GST or GST-EDS1 protein. Immunoprecipitated fractions were detected by anti-His and anti-GST antibodies, respectively. (D) Co-IP showing the interaction of EIJ1 and EDS1 in leaves of Arabidopsis. Total proteins extracted from 3-week-old $35S_{pro}$:*EIJ1-6HA* (as a genotype control) and $35S_{pro}$:*EIJ1-6HA* $35S_{pro}$:*EDS1-3FLAG* leaves were immunoprecipitated by either an anti-FLAG antibody or a preimmune serum (IgG). The coimmunoprecipitated proteins were detected using anti-FLAG and anti-HA antibodies, respectively. The representative results presented in (B–D) were repeated independently three times.

(*A. thaliana*) ecotype Columbia (Col-0; wild-type) plants by inoculation with *Pst* DC3000. Assessment of the infected leaves at 5-day post inoculation (dpi) revealed fewer necrotic lesions on *eij1-1* leaves than on Col-0 leaves (Figure 3D). Consistently, *eij1-1* leaves showed a significantly lower bacterial titer than Col-0 leaves at 5 dpi, although the bacterial titer showed no difference between Col-0 and *eij1-1* leaves at 0 dpi (Figure 3E).

Next, we generated *eij1-1* $EIJ1_{pro}$:*EIJ1-6HA* complementation lines by transforming a *EIJ1* genomic fragment fused with a 6xHA tag sequence into the *eij1-1* background. The complementation lines completely rescued the pathogen-resistance phenotype of *eij1-1* (Figure 3E), supporting that *eij1-1* is a loss-of-function mutant. To determine the effect of *EIJ1* on apoplastic immunity, the disease resistance phenotype of these complementation lines was also evaluated by pressure infiltration of *Pst* DC3000, and similar results were obtained (Supplemental Figure 4A). To confirm the function of *EIJ1*, we then identified another Arabidopsis mutant *eij1-2* (WiscDsLox343G09), which contained a T-DNA insertion in the promoter region of *EIJ1* (Supplemental Figure 5, A and B). The *EIJ1* transcripts were barely detectable in the *eij1-2* mutant, indicating that *eij1-2* is a null allele of *EIJ1*. Similar to *eij1-1*, bacterial growth assays revealed that *eij1-2* was present at a significantly lower bacterial titer than was Col-0 (Supplemental Figure 5, D and E). In summary, these results indicate that EIJ1 plays an important repressive role in the plant immune response.

The production of hydrogen peroxide (H_2O_2), a type of reactive oxygen species, is a hallmark of the successful recognition of pathogens and subsequent activation of plant defense responses, including HR-related programmed cell death

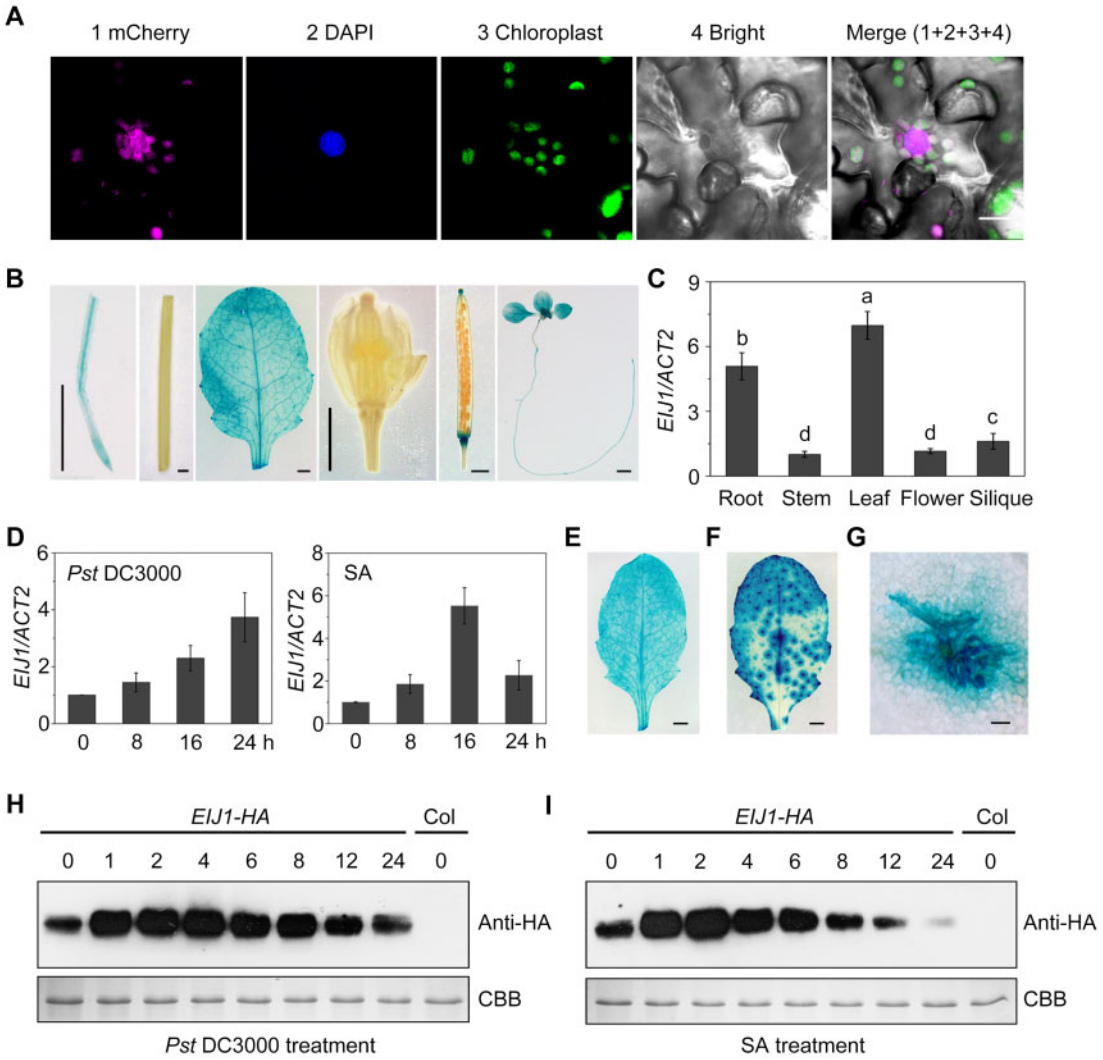

Figure 2 Expression pattern of EIJ1 mRNA and protein. (A) Chloroplast and nucleus localization of EIJ1. An EIJ1-mCherry fusion protein was transiently expressed in *N. benthamiana* leaves and analyzed by confocal microscopy. DAPI fluorescence indicates the nucleus. Chlorophyll fluorescence is indicated as green color. Bar = 10 μm. (B) GUS staining showing the expression of *EIJ1* in roots, stems, rosette leaves, flowers, siliques, and 10-day-old seedlings (from left to right). Bar = 1 mm. (C) Expression pattern of *EIJ1* in various tissues of Col plants including roots, stems, rosette leaves, flowers, and siliques, as detected by qRT-PCR. The relative expression was calculated by normalizing the transcription level of the examined gene against that of *ACTIN2* (the same below). The data are the mean ± SD of three biological replicates. Lowercase letters indicate significant differences (one-way ANOVA, $P < 0.01$; Supplemental Data Set 1). (D) Expression analysis of *EIJ1* using 3-week-old Col plants dip-inoculated with *Pst* DC3000 (OD_{600} = 0.1) or sprayed with 0.05 mM SA. The data are the mean ± SD of three biological replicates (Supplemental Data Set 1). (E–G) GUS staining showing the induction of *EIJ1* expression by pathogens. Three-week-old *pEIJ1:EIJ1-GUS* plants were mock inoculated (10 mM $MgCl_2$; E) or dip-inoculated with *Pst* DC3000 (OD_{600} = 0.1; F). Bar = 1 mm. Enlarged picture indicates that EIJ1-GUS concentrates at the trichome region in (G). Bar = 100 μm. Leaves at 4 hpi were harvested and incubated with GUS staining solution. (H) and (I) Expression pattern of EIJ1 following *Pst* DC3000 or SA treatment. Total proteins were extracted from 3-week-old $35S_{pro}$*:EIJ1-6HA* plants dip-inoculated with *Pst* DC3000 (OD_{600} = 0.1; H) or sprayed with 0.05 mM SA (I), and detected using an anti-HA antibody. The bottom panels show staining with Coomassie Brilliant Blue (CBB) as a loading control. The immunoblot analyses presented in (H) and (I) were repeated independently three times.

(Lam et al., 2001; Torres et al., 2006; Nanda et al., 2010). Therefore, we monitored the level of H_2O_2 in 3-week-old pathogen-inoculated Col-0, *eij1-1*, and *eij1-1* $EIJ1_{pro}$*:EIJ1-6HA* plants using the 3,3-diaminobenzidine (DAB) staining method. The results showed that H_2O_2 accumulated to high levels in the infected plants but was not detected in the uninoculated (mock) plants (Figure 3F). A higher level of H_2O_2 was detected in *eij1-1* leaves than in the leaves of Col-0 and complementation lines inoculated with *Pst* DC3000 (Figure 3F). Furthermore, while trypan-blue staining revealed that cell death (microHR, Alvarez et al., 1998) occurred in the *eij1-1* leaves at 24-h post inoculation (hpi) with *Pst* DC3000, but no microHR was observed in Col-0 and *eij1-1* $EIJ_{pro}1$*:EIJ1-6HA* plants (Figure 3G). Inoculation with avirulent *Pst* DC3000 (AvrRps4) resulted in higher accumulation of H_2O_2 and more microHR, although no visible difference was

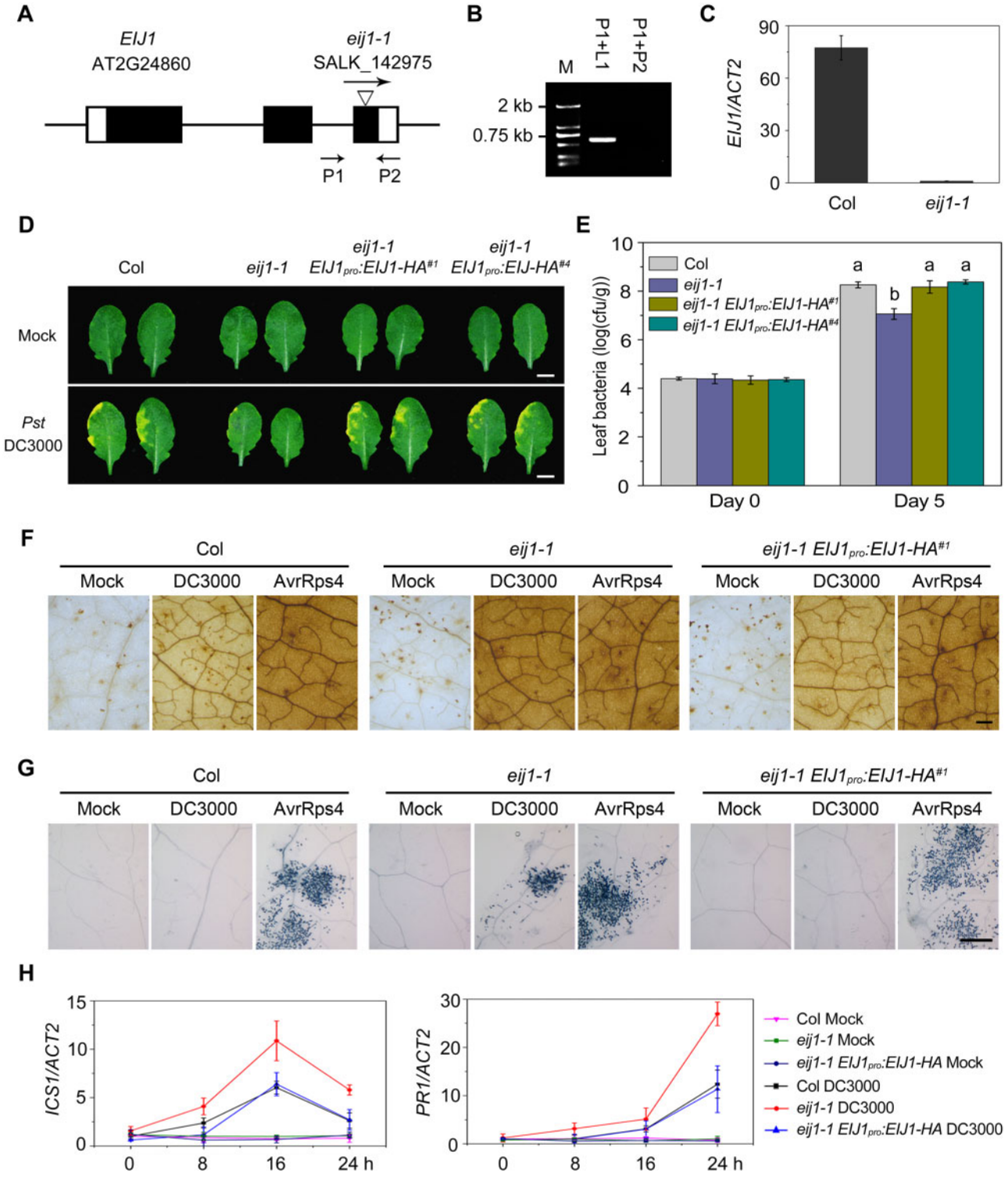

Figure 3 Identification of the Arabidopsis *EIJ1* mutated allele *eij1-1*. (A) Schematic diagram showing the T-DNA insertion site in *eij1-1* (SALK_142975). Exons are represented by boxes and introns by lines between the boxes. Black boxes present the *EIJ1* coding regions, and white boxes represent the untranslated region. Triangle indicates insertion site of T-DNA. (B) PCR amplification of genomic DNA confirms that *eij1-1* is a homozygous insertion mutant. The primers used (P1, P2) are shown in (A). LB indicates the T-DNA left border primer and M indicates the DNA molecular markers. (C) qRT-PCR analysis of *EIJ1* expression. Total RNA was extracted from 3-week-old *eij1* and Col leaves. The relative expression of *EIJ1* in *eij1-1* was set to 1. The data are the mean ± SD of three biological replicates (Supplemental Data Set 1). (D) The disease resistance phenotype of Col, *eij1-1*, and two representative *EIJ1* complementation transgenic lines *eij1 EIJ1*$_{pro}$*:EIJ1-6HA*. Three-week-old plants were dip-inoculated with *Pst* DC3000 (OD_{600} = 0.05). The leaves shown were photographed at 5 dpi. Bars = 5 mm. (E) Bacterial growth of *Pst* DC3000 on plants described in (D) at 0 and 5 dpi. cfu/g, colony forming units per g fresh weight. The data are the mean ± SD of three biological replicates. Lowercase letters indicate significant differences (one-way ANOVA, $P < 0.01$, Supplemental Data Set 1). (F) Examination of H_2O_2 levels in leaves of Col,

observed among these three genotypes (Figure 3, F and G). These results implied an essential role of *EIJ1* in basal resistance to pathogens.

SA is a major signaling molecule implicated in the resistance to biotrophic pathogens (Loake and Grant, 2007; An and Mou, 2011). Upon *Pst* DC3000 inoculation, the expression of *ICS1* (a SA biosynthetic gene) and *PATHOGENESIS-RELATED 1* (*PR1*; SA-responsive gene) was markedly upregulated in *eij1-1* compared to Col-0 plants and complementation lines (Figure 3H). Also, *PR1* expression was induced later than that of *ICS1* (Figure 3H), probably because PR1 functions downstream of ICS1-mediated SA biosynthesis. These results, together with the effect of SA on *EIJ1* expression (Figure 2, D and I), indicate that *EIJ1* plays a negative role in plant immune response via the SA pathway.

EIJ1 mediates plant immunity by repressing EDS1 activity

To understand the genetic relationship between *EDS1* and *EIJ1*, we generated *eij1-1 eds1-22* double mutant lines by crossing the *eij1-1* mutant with *eds1-22*, a loss-of-function mutant allele of *EDS1-90* (AT3G48090; Col-0 background), which exhibits compromised pathogen resistance (Yang and Hua, 2004). No morphological difference was observed among *eij1-1*, *eds1-22*, and *eij1-1 eds1-22* mutant plants under normal growth conditions (Figure 4, A and B). Following inoculation with *Pst* DC3000, the *eij1-1* mutant plants displayed stronger resistance than Col-0 plants at 5 dpi (Figure 4, A and B). However, the *eij1-1 eds1-22* double mutant presented remarkable necrotic lesions and high bacterial titer, comparable with the *eds1-22* single mutant, indicating that the *eij1-1* allele was unable to rescue the disease susceptible phenotype of *eds1-22* (Figure 4, A and B). Disease resistance was also evaluated following pressure infiltration of *Pst* DC3000, and similar results were obtained (Supplemental Figure 4B). Furthermore, we used the *EDS1* null allele, *eds1-2*; Col-0 background; Bartsch et al., 2006), to generate the *eij1-1 eds1-2* double mutant plants for genetic analysis. Similar to *eij1-1 eds1-22*, the *eij1-1 eds1-2* double mutant plants also showed remarkable necrotic lesions and higher bacterial titer than *eij1-1*, which was comparable with the *eds1-2* single mutant (Supplemental Figure 6). These genetic evidences suggest that *EDS1* is epistatic to *EIJ1*.

Consistent with the above observations, H_2O_2 accumulated to high levels in *eij1-1* leaves but to low levels in *eds1-22* and *eij1-1 eds1-22* leaves, compared with Col-0 leaves, upon *Pst* DC3000 inoculation (Figure 4C). Furthermore, microHR in *eij1-1* was clearly suppressed by the loss-of-function of *EDS1* at 24 hpi with *Pst* DC3000 or avirulent *Pst* DC3000 (AvrRps4; Figure 4D). Consistent with this result, the expression levels of *ICS1* and *PR1* in *eij1-1 eds1-22* and *eds1-22* plants were comparable but substantially lower than those in *eij1-1* and Col-0 plants (Figure 4E). These results support that EIJ1-mediated innate immune response is dependent on EDS1.

To investigate the role of EIJ1–EDS1 interaction in the plant immune response, we preformed RNA-seq analysis of *eij1-1*, *eds1-22*, and Col-0 leaves at 24 hpi with *Pst* DC3000; with uninoculated Col-0 leaves were used as a mock treatment. A total of 2762, 923, and 622 differentially expressed genes (DEGs) were identified in Col_*Pst* DC3000 versus Col_mock, *eij1-1*_*Pst* DC3000 versus Col_*Pst* DC3000, and *eds1-22*_*Pst* DC3000 versus Col_*Pst* DC3000 comparisons. These genes are hereafter referred to as pathogen-responsive, EIJ1-regulated, and EDS1-regulated genes, respectively (Supplemental Figure 7A and Data Set 2). Among these genes, 471 were regulated by EIJ1; 396 were regulated by EDS1 (Figure 4F; Supplemental Data Set 2); and 124 were co-regulated by EIJ1 and EDS1 (Figure 4F). Cluster analysis showed that 93.5% (116) of the co-regulated genes (124) were up-regulated by EDS1 and down-regulated by EIJ1 (Figure 4F; Supplemental Figure 7B and Data Set 2), supporting the repressive role of EIJ1 on EDS1 function. Gene ontology (GO) analysis further revealed that most of the genes regulated antagonistically by EIJ1 and EDS1 are mainly involved in stress responses and innate immune responses (Figure 4G; Supplemental Table S1). These analyses suggest that EIJ1 and EDS1 regulate resistance-related genes in a contrasting manner during pathogen infection. A considerable portion of the EDS1-regulated genes (272/396) were not regulated by EIJ1, probably because of the lower fold change (<2) or EIJ1-independent function of EDS1.

EIJ1 interacts with EDS1 in the cytoplasm and inhibits the nuclear trafficking of EDS1

EIJ1 is localized to the chloroplast and nucleus of leaf cells (Figure 2A), whereas EDS1 protein exhibits a nucleo-cytoplasmic distribution pattern, occurring in both places (García et al., 2010). To investigate where and how EIJ1 interacts with EDS1 in planta, we performed transient expression assays using Arabidopsis protoplasts. Interestingly, although EIJ1 maintained its original subcellular localization pattern in the chloroplast and nucleus in the presence

Figure 3 (Continued)
eij1-1, and the *eij1-1 EIJ1*$_{pro}$*:EIJ1-6HA*$^{\#1}$ complementation transgenic plants. Three-week-old plants were dip-inoculated with *Pst* DC3000 (OD_{600} = 0.1) or *Pst* DC3000 (AvrRps4; OD_{600} = 0.1), and then stained with 3,3-DAB at 24 hpi. Bar = 500 μm. (G) Cell death analysis of Col, *eij1-1*, and the *eij1-1 EIJ1*$_{pro}$*:EIJ1-6HA*$^{\#1}$ complementation transgenic plants. Three-week-old plants were dip-inoculated with *Pst* DC3000 (OD_{600} = 0.1) or *Pst* DC3000 (AvrRps4; OD_{600} = 0.1), and then stained with trypan blue at 24 hpi. The representative leaves presented in (F) and (G) were from six plants per genotype and the experiments were repeated independently three times. Bar = 500 μm. (H) qRT-PCR analysis of *ICS1* and *PR1* expression in Col, *eij1-1*, and the *eij1-1 EIJ1*$_{pro}$*:EIJ1-6HA*$^{\#1}$ complementation transgenic plants dip-inoculated with *Pst* DC3000 (OD_{600} = 0.1) or mock inoculated. Relative gene expression is shown as $\log_2$-transformed data. The data are the mean ± SD of three biological replicates (Supplemental Data Set 1).

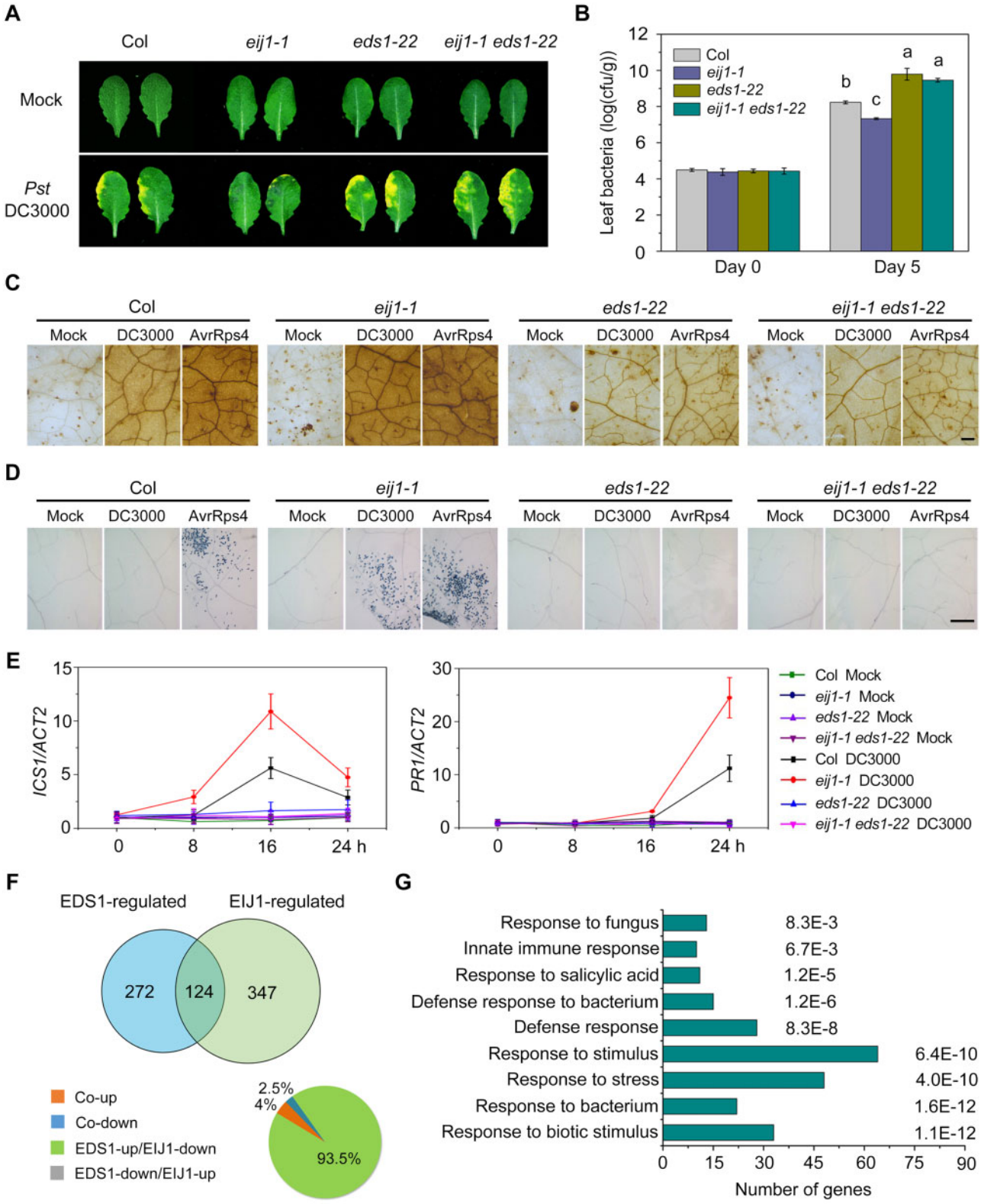

Figure 4 EIJ1 and EDS1 oppositely regulate plant resistance to pathogens. (A) The disease resistance phenotype of Col, *eij1-1*, *eds1-22*, and *eij1-1 eds1-22*. Three-week-old plants were dip-inoculated with *Pst* DC3000 (OD_{600} = 0.05). The leaves shown were photographed at 5 dpi. Bar = 5 mm. (B) Bacterial growth of *Pst* DC3000 on plants described in (A) at 0 and 5 dpi. The data are the mean ± SD of three biological replicates. Lowercase letters indicate significant differences (one-way ANOVA, $P < 0.01$, Supplemental Data Set 1). (C) Examination of H_2O_2 levels in Col, *eij1-1*, *eds1-22*, and *eij1-1 eds1-22* plants. Three-week-old plants were dip-inoculated with *Pst* DC3000 or *Pst* DC3000 (AvrRps4; OD_{600} = 0.1), and then stained with DAB at 24 hpi. Bar = 500 μm. (D) Cell death analysis of Col, *eij1-1*, *eds1-22*, and *eij1-1 eds1-22* plants. Three-week-old plants were dip-inoculated with *Pst* DC3000 or *Pst* DC3000 (AvrRps4; OD_{600} = 0.1), and then stained with trypan blue at 24 hpi. Bar = 500 μm.

of the green fluorescent protein (GFP; control), the chloroplast-localized EIJ1-mCherry was diffused in the cytoplasm when coexpressed with *EDS1-GFP* in protoplasts (Figure 5A, see replicates in Supplemental File 2). This phenomenon was confirmed in *N. benthamiana* epidermal cells, in which *EIJ1-mCherry* was transiently co-expressed with either *EDS1-GFP* or the *GFP* control (Supplemental Figure 8, see replicates in Supplemental File 2). These observations indicate that *EDS1* overexpression may lead to the subcellular relocalization of EIJ1. Next, to determine the subcellular location where EDS1 and EIJ1 interact, we performed a pull-down assay using the recombinant Glutathione S-Transferase (GST)-EDS1 fusion protein (bait) and total protein extract, nuclei-depleted fractions, and nuclei-enriched fractions of $35S_{pro}$:*EIJ1-HA* transgenic lines (prey proteins). Our results showed that EDS1 immunoprecipitated with EIJ1-HA when using the total protein extract and nuclei-depleted fractions of $35S_{pro}$:*EIJ1-HA* leaves, but it did not when using the nuclei-enriched fractions (Figure 5B), suggesting that the interaction between EIJ1 and EDS1 occurs in the cytoplasm.

Given that EIJ1 negatively regulates plant immune response in an EDS1-dependent manner (Figure 4), we next examined the effect of pathogens on the interaction between EIJ1 and EDS1. Surprisingly, *Pst* DC3000 infection enhanced the EDS1–EIJ1 interaction in the cytoplasm rather than in both the chloroplast and nucleus (Figure 5C, see replicates in Supplemental File 2). This finding, together with the nucleo-cytoplasmic distribution pattern of EDS1 and the role of EDS1 nuclear localization in the reinforcement of pathogen resistance at the transcriptional level (García et al., 2010), compelled us to investigate the role of EIJ1 in the subcellular trafficking of EDS1 during pathogen infection. When we transiently expressed *EDS1-3FLAG* in Arabidopsis protoplasts isolated from *eij1-1*, *EIJ1* overexpression, and Col-0 plants, EIJ1 notably repressed the trafficking of EDS1 into the nucleus (Supplemental Figure 9). Furthermore, immunoblot analysis revealed that little difference in the abundance of total EDS1 protein between *eds1-22* $EDS1_{pro}$:*EDS1-3FLAG* and *eij1-1 eds1-22* $EDS1_{pro}$:*EDS1-3FLAG* transgenic plants (Figure 5D, see replicates in Supplemental File 2). However, compared with *eds1-22* $EDS1_{pro}$:*EDS1-3FLAG* transgenic plants, *Pst* DC3000-inoculated *eij1-1 eds1-22* $EDS1_{pro}$:*EDS13FLAG* plants showed a marked increase in the level of nuclei-enriched EDS1 protein and a reduction in the level of cytoplasm-localized EDS1 (Figure 5D, see replicates in Supplemental File 2), confirming the repressive role of EIJ1 in the cytoplasm-to-nucleus trafficking of EDS1.

Next, we tested whether this redistribution process mediated by the EIJ1–EDS1 interaction affected the transcriptional regulation of resistance-related genes in plants. The $35S_{pro}$:*EIJ1-mCherry* and $35S_{pro}$:*EDS1-3FLAG* effector constructs were transformed individually or together with the reporter construct into *N. benthamiana* leaf epidermal cells (Figure 5E). At 24 hpi with *Pst* DC3000, EDS1 activated the expression of *PR1* and *ICS1* (Figure 5F), while EIJ1 markedly inhibited EDS1-induced gene expression (Figure 5F). Unlike the full-length EIJ1, the N-terminal end of the EIJ1 protein, which is unaffected in *eij1-1*, was unable to inhibit the EDS1-induced *PR1* expression (Supplemental Figure 10, A and B), indicating that the intact protein structure of EIJ1 is necessary for its repressive function. Together, these results support that EIJ1 functions as an essential repressor in EDS1-mediated resistance response by regulating the nucleo-cytoplasmic trafficking of EDS1.

Because the EIJ1 protein was gradually degraded in *Pst* DC3000-inoculated or SA-treated plants after a quick initial induction (Figure 2, H and I), we investigated whether EDS1 in turn triggers the degradation of EIJ1 via a protein–protein interaction. Cell-free degradation assays and in vivo protein detection assays using *eds1-22* $35S_{pro}$:*EIJ1-HA* transgenic plants showed that neither the absence nor the presence of EDS1 affected EIJ1 degradation (Supplemental Figure 11), suggesting that EDS1 is not involved in the pathogen-triggered degradation of EIJ1.

Pathogen infection alters the subcellular localization of EIJ1

The enhanced interaction between EIJ1 and EDS1 in the cytoplasm upon pathogen inoculation (Figure 5, B and C) implied a possible pathogen-triggered relocalization of EIJ1 in plant cells. To test this possibility, we examined the subcellular localization of EIJ1 in *N. benthamiana* leaves inoculated with *Pst* DC3000. Under uninfected conditions, EIJ1-mCherry was localized to the chloroplast and nucleus. However, at 24 hpi, the fluorescence signals were greatly decreased in the chloroplasts and were enhanced in the cytoplasm (Figure 6A). To further determine whether pathogens trigger the disassociation of EIJ1 from the chloroplast to the cytoplasm in leaves, immunoblot analysis of EIJ1 protein was performed using $35S_{pro}$:*EIJ1-6HA* transgenic plants. Total proteins, chloroplast proteins, and cytoplasmic proteins were isolated from $35S_{pro}$:*EIJ1-6HA* transgenic plants at 0 and 4 hpi with *Pst* DC3000. The abundance of EIJ1 was remarkably

Figure 4 (Continued)
The representative leaves presented in (C) and (D) were from six plants per genotype and the experiments were repeated independently three times. (E) qRT-PCR analysis of *ICS1* and *PR1* expression in Col, *eij1-1*, *eds1-22*, and *eij1-1eds1-22* plants challenged with *Pst* DC3000 (OD_{600} = 0.1) or given a mock dip inoculation. The data are the mean ± SD of three biological replicates (Supplemental Data Set 1). (F) Venn diagram showing the overlapped genes coregulated by EIJ1 and EDS1 in transcriptomic analysis, and the lower pie chart showing the co-upregulated, co-downregulated, and oppositely regulated genes by EIJ1 and EDS1. No gene upregulated by EIJ1 and downregulated by EDS1 (gray color) was found. The DEGs were identified with the criteria: *q*-value <0.0001 and fold change >2. (G) GO analysis of genes coregulated by EIJ1 and EDS1. The bar indicates gene number in each category.

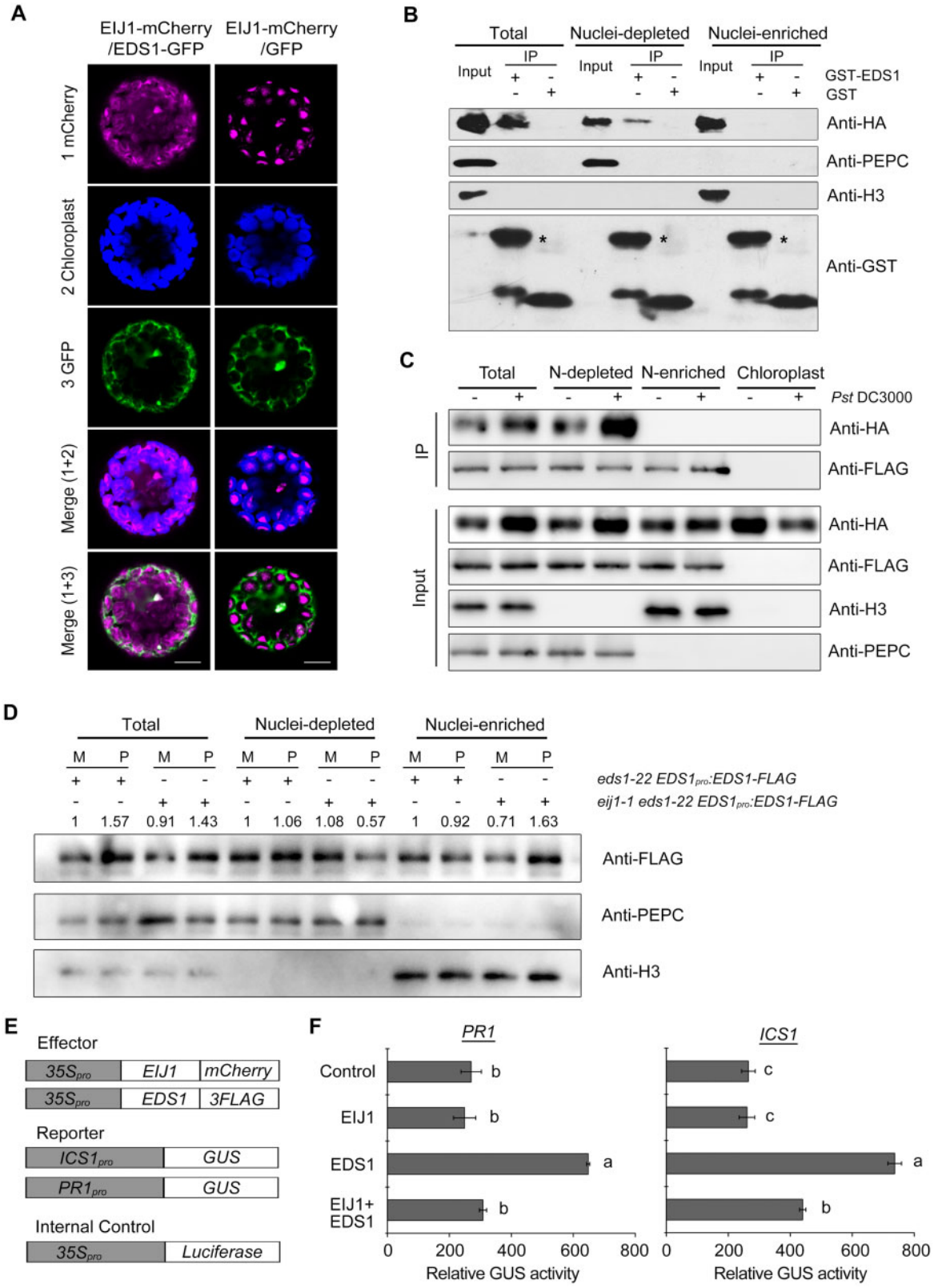

Figure 5 EIJ1 Interacts with EDS1 in the cytoplasm to mediate nuclear trafficking of EDS1. (A) Transient expression analysis showing the localization of EDS1 and EIJ1 in Arabidopsis protoplasts. Bar = 10 μm. (B) Pull-down assay of interaction between EIJ1 and EDS1. Total proteins, nuclei-depleted fractions, and nuclei-enriched fractions extracted from 3-week-old *eij1-1* $35S_{pro}$*:EIJ1-6HA* transgenic plants were incubated with immobilized GST-EDS1 or GST proteins, respectively. IPs were detected using anti-HA or anti-GST antibodies. PEPC and histone H3 were used as cytoplasmic and nuclear markers, respectively. Asterisks indicate the bands of GST-EDS1 proteins. (C) *Pst* DC3000 infection enhances the protein interaction of EDS1 and EIJ1 in the cytoplasm. Total proteins, nuclei-depleted fractions, nuclei-enriched fractions, and chloroplast proteins were

increased in the cytoplasmic fraction but decreased in the chloroplast fraction at 24 hpi (Figure 6B, see replicates in Supplemental File 2), indicating a negative correlation between the EIJ1 protein levels in the chloroplast and cytoplasm.

Pathogen-triggered EIJ1 dissociation from the chloroplast suggests a potential function of EIJ1 in the cytoplasm. To test this possibility, we immobilized the EIJ1 protein onto the chloroplasts by attaching the chloroplast-targeting sequence (CTS; Lee et al., 2008) to the N-terminal end of the *EIJ1-mCherry* reporter gene. The *CTS-EIJ1-mCherry* fusion was then expressed in *N. benthamiana* leaves under the control of the native promoter. Fluorescence was detected only in the chloroplasts, but not in the cytosol and nucleus of *Pst* DC3000-inoculated *N. benthamiana* leaves (Supplemental Figure 12A). This observation confirmed that the CTS-tagged EIJ1 was retained in the chloroplast and not forced into the cytoplasm by pathogen infection. We subsequently generated *EIJ1*$_{pro}$*:CTS-EIJ1-6HA* transgenic Arabidopsis lines to evaluate the biological function of CTS-EIJ1 in the plant immune response. As expected, unlike *eij1-1 EIJ1*$_{pro}$*:EIJ1-6HA*, the *eij1-1 EIJ1*$_{pro}$*:CTS-EIJ1-6HA* lines showed no significant difference in the resistance to pathogens compared with *eij1-1*, indicating that EIJ1 immobilized in the chloroplast is unable to rescue the disease resistance phenotype of *eij1-1* (Figure 6C). Consistent with this observation, the expression of *PR1* was maintained at a high level in *eij1-1 EIJ1*$_{pro}$*:CTS-EIJ1-6HA* transgenic plants, similar to *eij1-1* (Supplemental Figure 12B). In addition, CTS-EIJ1 exhibited less ability to repress EDS1 transcription activity than EIJ1 (Figure 6, D and E). These results led us to conclude that an early host response to pathogen infection triggers the subcellular relocalization of EIJ1, which in turn modulates the immune response by repressing the trafficking of EDS1 into the nucleus.

EIJ1 regulates the virulence effector-triggered response

The AvrRps4 effector protein of *P. syringae* secreted by the type III secretion system is recognized by the TIR-NB-LRR receptor RPS4 to initiate ETI, which is dependent on EDS1 (Gassmann et al., 1999; Wirthmueller et al., 2007; Heidrich et al., 2012). We inoculated *eij1-1* leaves with the avirulent *Pst* DC3000 (AvrRps4) or virulent *Pst* DC3000 to assess whether EIJ1 is involved in ETI. The *eij1-1* leaves showed greater resistance to virulent *Pst* DC3000 than did Col-0 leaves (Figure 7A). However, no significant difference was observed between Col-0 and *eij1-1* leaves in resistance to avirulent *Pst* DC3000 (AvrRps4), although both genotypes showed greater resistance to avirulent *Pst* DC3000 (AvrRps4) than to *Pst* DC3000 (Figure 3, F and G; Figure7, A), indicating that *EIJ1* may not be necessary for RPS4-induced ETI. We also determined the resistance of plants to *Pst* DC3000 *hrcC*, which harbors a defective type III secretion system and fails to inject effectors into host cells to suppress PTI (Gassmann et al., 1999; Gloggnitzer et al., 2014). Both the *eij1-1* mutant and Col-0 leaves showed similar resistance to *Pst* DC3000 *hrcC* (Supplemental Figure 13), suggesting that EIJ1 is not involved in PTI.

Given that the nuclear accumulation of EDS1 is indispensable for the TIR-NB-LRR-induced reprogramming of defense gene expression and resistance (García et al., 2010), we examined whether EIJ1 regulates the subcellular distribution of EDS1 in response to ETI. Leaves of 3-week-old *eds1-22 EDS1*$_{pro}$*:EDS1-3FLAG* and *eij1-1 eds1-22 EDS1*$_{pro}$*:EDS1-3FLAG* plants were inoculated with either *Pst* DC3000 or *Pst* DC3000 (AvrRps4), and the nuclei-depleted and nuclei-enriched fractions were extracted at 0 and 4 hpi. Consistent with the previous study (García et al., 2010), an increase in nuclear localization of EDS1 was observed in *eds1-22 EDS1*$_{pro}$*:EDS1-3FLAG* plants inoculated with *Pst* DC3000 (AvrRps4), but not in those inoculated with *Pst* DC3000. However, the loss-of-function of *EIJ1* did not affect the ETI-induced nuclear accumulation of EDS1 (Figure 7B; see replicates in Supplemental File 2). This suggests that the avirulent *Pst* DC3000 (AvrRps4) either triggers the trafficking of EDS1 into the nucleus by bypassing EIJ1 or abolishes the function of EIJ1 in an unknown manner.

To test these possibilities, we examined the effect of avirulent *Pst* DC3000 (AvrRps4) on the level of EIJ1. Similar to the results obtained using *EIJ1* overexpression lines (Figure 2H), the *eij1-1 EIJ1*$_{pro}$*:EIJ1-6HA* plants inoculated with *Pst* DC3000 showed increased EIJ1 accumulation at an early

Figure 5 (Continued)

extracted from 3-week-old *EIJ1*$_{pro}$*:EIJ1-6HA 35S*$_{pro}$*:EDS1-3FLAG* plants dip-inoculated with *Pst* DC3000 (OD_{600} = 0.1) or mock inoculated at 4 hpi, and immunoprecipitated using either an anti-FLAG antibody or a preimmune serum (IgG). The co-immunoprecipitated proteins were detected using anti-HA and anti-FLAG antibodies. N-depleted, nuclei-depleted fractions; N-enriched, nuclei-enriched fractions. PEPC and histone H3 were used as cytoplasmic and nuclear markers, respectively. (D) Immunoblot analysis showing that EIJ1 mediates the cytoplasmic versus nuclear distribution of EDS1. Total proteins, nuclei-depleted fractions, and nuclei-enriched fractions were extracted from 3-week-old *eds1-22 EDS1*$_{pro}$*:EDS1-3FLAG* and *eij1-1 eds1-22 EDS1*$_{pro}$*:EDS1-3FLAG* transgenic plants dip-inoculated with *Pst* DC3000 (OD_{600} = 0.1) or mock inoculated at 4 hpi, and detected using an anti-FLAG antibody. The relative intensity of proteins from *eds1-22 EDS1*$_{pro}$*:EDS1-3FLAG* with the mock inoculation treatment set to 1. M, mock; P, *Pst* DC3000. PEPC and histone H3 were used as cytoplasmic and nuclear markers, respectively. The results presented in (A), (C), and (D) were repeated independently three times (Supplemental File 2). (E) and (F) Transient analysis of *PR1* and *ICS1* promoter activity regulated by EIJ1 and EDS1. Various constructs used in transient expression assays are shown in (E). Either *PR1*$_{pro}$*:GUS* or *ICS1*$_{pro}$*:GUS* was cotransformed with effectors or the empty vector (Control) into *N. benthamiana* leaves spayed with *Pst* DC3000 (OD_{600} = 0.1) for 24 h. Relative GUS activity (GUS/Luciferase) that indicates the expression level of *PR1* and *ICS1* regulated by various effectors is shown in (F). The data are the mean ± SD of three biological replicates (Supplemental Data Set 1). Lowercase letters indicate significant differences (one-way ANOVA, $P < 0.01$).

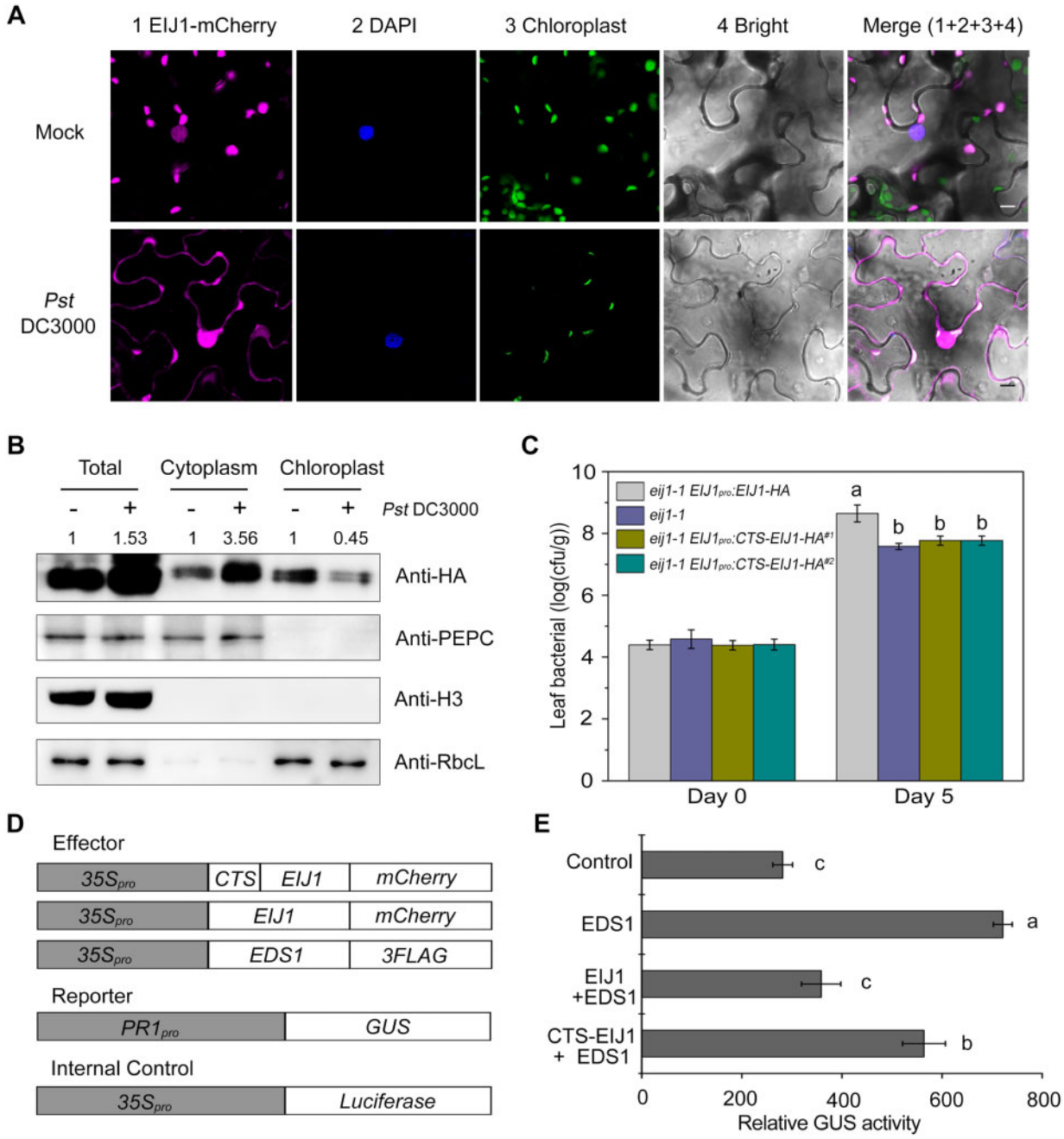

Figure 6 Relocalization of EIJ1 to the cytoplasm is necessary for EDS1-dependent resistance. (A) *Pst* DC3000 infection alters the subcellular localization of EIJ1. EIJ1-mCherry was transiently expressed in *N. benthamiana* leaves spayed with *Pst* DC3000 (OD_{600} = 0.1) or mock inoculated for 24 h. Bar = 10 μm. (B) *Pst* DC3000 infection triggers the disassociation of EIJ1 from the chloroplast. Total proteins, cytoplasmic proteins, and chloroplastic proteins were extracted from 3-week-old $EIJ1_{pro}$:*EIJ1-6HA* plants dip-inoculated with *Pst* DC3000 (OD_{600} = 0.1) or mock inoculated at 4 hpi, and detected by anti-HA antibody. PEPC, histone H3, and RbcL were used as cytoplasmic, nuclear, and chloroplastic markers, respectively. The relative intensity of proteins with mock treatment is set to 1. The results presented in (A) and (B) were repeated independently three times (Supplemental File 2). (C) Immobilized EIJ1 in chloroplasts is unable to restore the resistance of *eij1-1*. Three-week-old plants were dip inoculated with *Pst* DC3000 (OD_{600} = 0.05). Bacterial titer of *Pst* DC3000 at 0 and 5 dpi was determined. CTS, chloroplast localization signals. The data are the mean ± SD of three biological replicates (Supplemental Data Set 1). (D) and (E) Transient analysis of *PR* promoter activity regulated by EIJ1, CTS-EIJ1, and EDS1. Various constructs used in transient expression assays are shown in (D). $PR1_{pro}$:*GUS* was co-transformed with effectors or the empty vector (Control) into *N. benthamiana* leaves spayed with *Pst* DC3000 (OD_{600} = 0.1) for 24 h. Relative GUS activity (GUS/Luciferase) that indicates the expression level of *PR1* regulated by various effectors is shown in (E). Error bars represent standard deviation of triplicate independent samples. The data are the mean ± SD of three biological replicates. Lowercase letters indicate significant difference (one-way ANOVA, $P < 0.01$, Supplemental Data Set 1).

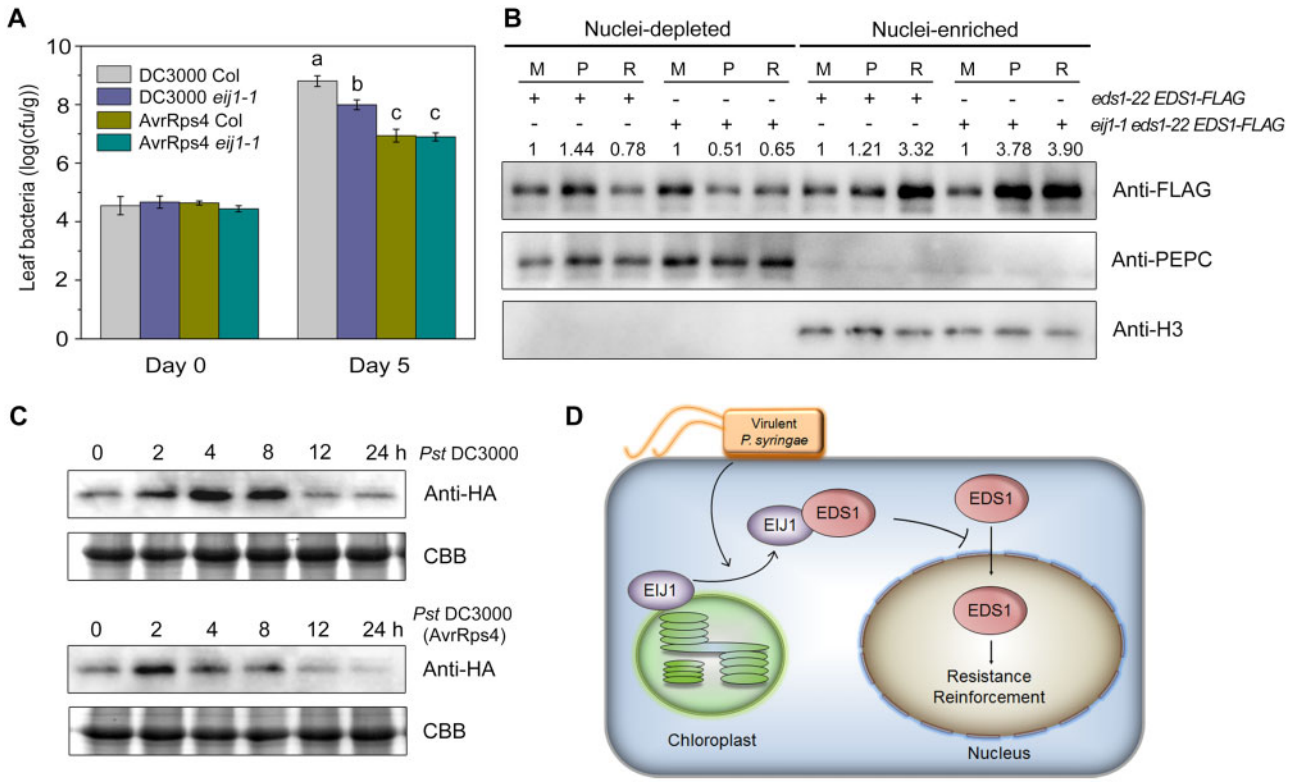

Figure 7 EIJ1 and EDS1 modulate plant basal resistance. (A) Bacterial growth of Col and *eij1-1* mutant. Three-week-old plants were dip inoculated with *Pst* DC3000 or *Pst* DC3000 (AvrRps4; OD_{600} = 0.05). Bacterial titer of *Pst* DC3000 at 0 and 5 dpi was determined. The data are the mean ± SD of three biological replicates. Lowercase letters indicate significant difference (one-way ANOVA, $P < 0.01$, Supplemental Data Set 1). (B) EIJ1 hardly affects *Pst* DC3000 (AvrRps4)-triggered accumulation of EDS1 in nuclei. Nuclei-depleted fractions and nuclei-enriched fractions were extracted from 3-week-old *eds1-22 EDS1*$_{pro}$*:EDS1-3FLAG* and *eij1-1 eds1-22 EDS1*$_{pro}$*:EDS1-3FLAG* transgenic plants dip inoculated with *Pst* DC3000 (OD_{600} = 0.1), *Pst* DC3000 (AvrRps4; OD_{600} = 0.1), or mock inoculated at 4 hpi, and detected using an anti-FLAG antibody. PEPC and histone H3 were used as cytoplasmic and nuclear markers, respectively. The relative intensity of proteins from plants with mock treatment was set to 1. M, mock; P, *Pst* DC3000; R, *Pst* DC3000 (AvrRps4). (C) *Pst* DC3000 (AvrRps4) infection promotes the degradation of EIJ1 protein. Total proteins were extracted from 3-week-old *eij1-1 EIJ1*$_{pro}$*:EIJ1-6HA* plants dip-inoculated with *Pst* DC3000 or *Pst* DC3000 (AvrRps4; OD_{600} = 0.1), and detected using an anti-HA antibody. The bottom panel shows staining with Coomassie Brilliant Blue (CBB) as a loading control. The representative results presented in (B) and (C) were repeated independently two more times and probed with an anti-ACTIN antibody as a loading control (Supplemental File 2). (D) Hypothetical model of EIJ1 regulating EDS1-dependent plant basal resistance. When plants are invaded by pathogens, EIJ1 is rapidly released from the chloroplast into the cytoplasm where it interacts with EDS1. The EIJ1–EDS1 interaction prevents the shuttling of EDS1 from the cytoplasm into the nucleus and thus restricts the nuclear resistance of EDS1, allowing the modulation of EDS1-mediated immune responses. Arrowed and blunted lines indicate activation and repression, respectively.

stage of infection, although EIJ1 was gradually degraded after 8 hpi (Figure 7C; see replicates in Supplemental File 2). The accumulation of EIJ1 is sufficient to prevent the *Pst* DC3000-triggered trafficking of EDS1 into the nucleus at an early infection stage (Figures 5, D and 7, B). Consistent with this result, the loss-of-function of *EIJ1* accelerated the nuclear translocation of EDS1 in infected plants (Supplemental Figure 14). In contrast, *Pst* DC3000 (AvrRps4) abolished EIJ1 function by rapidly inducing EIJ1 protein degradation, but not by repressing *EIJ1* gene transcription (Figure 7C; Supplemental Figure 15), thus promoting more nuclear translocation of EDS1 at the early stage of infection (Figure 7B). The observation that *eij1-1* plants inoculated with *Pst* DC3000 exhibited resistance comparable to that of Col-0 and *eij1-1* plants inoculated with the avirulent *Pst* DC3000 (AvrRps4) supports this hypothesis. This may explain, at least to some extent, why the avirulent strain, but not the virulent strain, can mount the reinforced resistance to trigger ETI response. Therefore, these observations suggest that EIJ1 is involved in virulence effector-triggered response in host cells.

Discussion

To maximize survival, plants have evolved a precise mechanism for optimizing growth and for defense against invading pathogens, although numerous details of these mechanisms remain unclear. EDS1 occupies a key position in the plant innate immunity signaling network, as it regulates resistance to biotrophic and hemibiotrophic pathogens (Wiermer et al., 2005). In this study, we identified a gene, *EIJ1*, which encodes a chaperone DnaJ protein, and showed that EIJ1 is

responsive to early pathogen infection and plays a role in plant innate immunity by interacting directly with EDS1. On the basis of these findings, we propose a regulatory model for EIJ1 (Figure 7D). When plants are invaded by pathogens, EIJ1 is rapidly released from the chloroplast to the cytoplasm, where it interacts with EDS1. This EIJ1–EDS1 interaction prevents the shuttling of EDS1 from the cytoplasm into the nucleus, and this restricts the nuclear resistance of EDS1, allowing the modulation of EDS1-mediated immune responses such as the induction of SA biosynthesis and expression of resistance-related genes. When plants suffer continuous stimuli from invading pathogens, EIJ1 is gradually degraded, leading to an increased nuclear accumulation of EDS1 for resistance reinforcement. These findings illustrate an essential repressive role of EIJ1 during the early host response to pathogen invasion, filling the gap in our understanding of how the subcellular localization of EDS1 is regulated to confer resistance.

Sequence analysis revealed that EIJ1 is a DnaJ protein. The Arabidopsis genome encodes seven different classical types of DnaJ proteins (Pulido and Leister, 2018). Previous studies show that DnaJ proteins play important and distinct roles in plant immunity. For instance, soybean (*Glycine max*) GmHSP40 positively regulates cell death and disease resistance (Liu and Whitham, 2013). In contrast, the rice (*Oryza sativa* L.) Os-DjA6 protein negatively regulates plant innate immunity through the ubiquitination-mediated proteasome degradation pathway (Zhong et al., 2018). The *P. syringae*-specific Hopl1 virulence effector, which contains a J domain, is targeted to the chloroplast, where it interacts with the plant stress–response machinery (Jelenska et al., 2007). These studies demonstrate that DnaJ proteins play diverse roles in plant defense response. Tsip1, a *N. tabacum* DnaJ protein homologous to EIJ1, regulates the *Tsi1*-mediated transcriptional activation of genes in response to stress (Ham et al., 2006). *Tsi1* encodes an APETALA2 (AP2)-type transcription factor that functions as an important regulator in both biotic and abiotic stress responses in *N. tabacum* (Park et al., 2001). SA triggers the relocalization of Tsip1 from the chloroplast to the cytoplasm, which facilitates the interaction between Tsip1 and Tsi1 and the subsequent entry of the Tsip1–Tsi1 complex into the nucleus for transcriptional activation of stress-related genes (Ham et al., 2006). Unlike Tsip1, EIJ1 was localized to the chloroplast and nucleus under normal conditions in this study. We showed that pathogen infection triggers the relocalization of EIJ1 from the chloroplast to the cytoplasm, and that the interaction between EIJ1 and EDS1 in the cytoplasm inhibits EDS1-mediated nuclear resistance. Consistent with this finding, the loss-of-function *eij1*mutant exhibited stronger resistance to pathogens than the wild-type (Col-0). This confirms that EIJ1 plays a negative role in plant innate immunity.

According to previous studies, coordinated nuclear and cytoplasmic activities of EDS1 are essential for plants to complete the innate immune response to pathogens (García et al., 2010; Heidrich et al., 2011). The nuclear localization of EDS1 is required for TNL-induced resistance transcriptional reprogramming to induce SA-related and other plant defense responses (Wirthmueller et al., 2007). The cytoplasmic EDS1 pool is also maintained during the infection process for complete resistance to pathogens (García et al., 2010). These observations raise a significant concern regarding how plants precisely regulate the allocation of EDS1 between the cytoplasm and nucleus for proper defense responses when challenged by pathogen infection. Here, we show that the precise allocation of EDS1 to different subcellular compartments is regulated in part by EIJ1 via protein–protein interaction. The loss-of-function mutation of *EIJ1* notably promoted the trafficking of EDS1 to the nucleus (Figures 5, D and 7, B), leading to enhanced disease resistance.

Because EIJ1 was rapidly induced at an early stage of pathogen infection and subsequently degraded during disease development, we speculate that EIJ1 is an important negative regulator of immunity that allows plants to refine their optimal defenses. The EIJ1-mediated repression of EDS1 activity could prevent elicitation of unnecessary immune responses to short-term stimulation such as an occasional attack by pathogenic bacteria. Alternatively, it is possible that pathogenic bacteria manipulate host immunity by triggering the disassociation of EIJ1 from the chloroplast, probably by secreting virulent effectors. We could not exclude the possibility that EIJ1 performs an unknown function in the chloroplast. As we know, SA, a plant hormone and signaling molecule implicated in the resistance to biotrophic pathogens, is biosynthesized primarily in the chloroplast and then exported out into the cytoplasm by EDS5, a multidrug and toxin transporter (Serrano et al., 2013). EIJ1 is likely a negative regulator of SA accumulation, as it down-regulated the expression of the SA biosynthetic gene *ICS1* upon pathogen inoculation (Figure 4E). In addition to the EIJ1-mediated transcriptional repression via its interaction with EDS1, it is possible that EIJ1 also plays a direct role in SA biosynthesis or SA transport from the chloroplast in an unidentified manner. It would not be surprising if EIJ1 and the SA biosynthesis process are found to be connected in a future study. Interestingly, EIJ1 was also localized to the nucleus. Although EIJ1 did not interact with EDS1 in nucleus, probably because of the lack of essential cofactors or modifications, the function of nucleus-localized EIJ1 is worthy of further investigation.

Pathogenic bacteria produce intracellular effectors to subvert the PTI of the host by targeting pathogen resistance proteins such as PRRs, whereas plant cytoplasmic NOD-like receptors sense these effectors to initiate ETI (Dou and Zhou, 2012; Khan et al., 2016). Previous studies and our results showed that avirulent *Pst* DC3000 (AvrRps4) promotes trafficking of the cytoplasmic EDS1 into the nucleus (García et al., 2010). Furthermore, our results showed no significant difference in *Pst* DC3000 (AvrRps4)-triggered nuclear accumulation of EDS1 and subsequent pathogen resistance between Col-0 and *eij1-1* mutant plants (Figure 7, A and B).

Additionally, the resistance exhibited by the *eij1-1* mutant was comparable to that exhibited by Col-0 plants inoculated with the type III secretion system-defective *Pst* DC3000 *hrcC* strain (Supplemental Figure 12). Moreover, the accumulation of EIJ1 was markedly lower in plants inoculated with avirulent *Pst* DC3000 (AvrRps4) than in plants inoculated with virulent *Pst* DC3000 (Figure 7C), indicating that EIJ1 is an essential regulator of virulence effector-triggered immune response in host cells. Because *Pst* DC3000-inoculated *eij1-1* plants mimicked the resistance phenotype of *Pst* DC3000 (AvrRps4)-inoculated Col-0 plants (Figures 3, F, G, 4, C, D, and 7, A), it is possible that EIJ1 functions as a barrier to prevent the induction of ETI by virulent strains.

In conclusion, we have identified EIJ1, a chaperone DnaJ protein, and showed that it is involved in an early immune response to plant pathogens. The interaction between EIJ1 and EDS1 represses the nuclear trafficking of EDS1, probably either to prevent short-term stimulation by unnecessary plant immune responses, or to facilitate the pathogenic invasion by a manipulating mechanism, or both. Regardless of the underlying mechanism, the *EIJ1* allele could be employed as an effective potential target for the modification of plant innate immunity in disease resistance breeding. Because EIJ1 does not affect the normal growth of plants, attenuation of EIJ1 function via genome editing might prominently elevate the level of disease resistance of crops with little effect on growth.

Material and Methods

Plant materials and growth conditions

All Arabidopsis plants used in this study are in the *A. thaliana* Col-0 background. The *eij1-1* (SALK_142975) mutant, *eij1-2* (WiscDsLox343G09) mutant, *eds1-22* (SALK_071051) mutant, *eds1-2* mutant (Bartsch et al., 2006), and all transgenic lines are described in Supplemental Table 2. All Arabidopsis plants were grown under short day conditions with 12-h light (100 μmol m^{-2} s^{-1}) and 12-h dark.

Plasmid construction and plant transformation

For the $35S_{pro}$:*EIJ1-6HA* and $35S_{pro}$:*EIJ1-mCherry* constructs, the coding region of *EIJ1* was cloned into *pGreen-35S-6HA* and *pGreen-35S-mCherry* (Li et al., 2019), respectively. For the $EIJ1_{pro}$:*EIJ1-6HA* and $EIJ1_{pro}$:*EIJ1-GUS* constructs, a ~1.5-kb genomic fragment of *EIJ1* was cloned into the *HY105-6HA* and *HY105-GUS* plasmids (Li et al., 2019), respectively. For the *EIJ1pro:CTS-EIJ1-6HA* and $EIJ1_{pro}$:*CTS-EIJ1-mCherry* constructs, a *CTS* encoding the MASSMLSSATMVASPA peptide (Lee et al., 2008) was attached to the N-terminus of *EIJ1*, and then cloned into *HY105-6HA* and *HY105-mCherry* plasmids, respectively. For the $35S_{pro}$:*EDS1-3FLAG* construct, the coding region of *EDS1* was cloned into *pZPY122-35S-3FLAG* (Li et al., 2019). For $EDS1_{pro}$:*EDS1-3FLAG* construct, a ~3.5-kb genomic fragment was cloned into *pGreen-3FLAG* (Li et al., 2019). Primers used for plasmid construction are listed in Supplemental Table 3. All Arabidopsis transgenic plants were selected on 1/2x Murashige and Skoog (MS) medium supplied with Basta (Kingbio, Cat# 2471) except that $35S_{pro}$:*EDS1-3FLAG* were selected with gentamycin.

Pathogen infection assay

The bacteria *Pst* DC3000, *Pst* DC3000 (AvrRps4) and *Pst* DC3000 *hrcC* were cultured in King's B medium (10 mg mL^{-1} protease peptone, 1.5 mg mL^{-1} K_2HPO_4, and 15 mg mL^{-1} glycerol) containing 25 mg mL^{-1} rifampicin [supplemented with 50 mg mL^{-1} kanamycin for *Pst* DC3000 {AvrRps4}] at 28°C. For observation of disease symptoms, 3-week-old plants were dip inoculated with *Pst* DC3000 (a suspension of OD_{600} = 0.05, equivalent to ~10^7 cfu mL^{-1}) or a mock suspension (10 mM $MgCl_2$; Melotto et al., 2006). The bacterial growth assays were also performed using an infiltration method as described (Yang et al., 2015), in which a *Pst* DC3000 (OD_{600} = 0.0002) suspension in 10 mM $MgCl_2$ was hand-infiltrated into leaves of 4-week-old plants. Ten infected leaves from each of five plants were collected to detect bacterial growth at 5 dpi. Leaf discs of each sample were collected and ground with a pestle in 1 mL of 10 mM $MgCl_2$. This material was diluted, and then cultured on King's B medium with rifampicin (Li et al., 2019). Six replicated samples per genotype were collected and statistically analyzed. For transcription and protein analysis, plants were dip inoculated with *Pst* DC3000 or *Pst* DC3000 (AvrRps4; OD_{600} = 0.1). For fluorescence analysis of *N. benthamiana* leaves, the plants were sprayed with *Pst* DC3000 (OD_{600} = 0.1) or mock inoculated (10 mM $MgCl_2$) for 24 h.

Histochemistry analysis

Three-week-old plants were dip inoculated with *Pst* DC3000 (OD_{600} = 0.1) or 10 mM $MgCl_2$. Leaves at 4 hpi were harvested and incubated with a GUS staining solution (50 mM Na_3PO_4 (pH 7.0), 0.5 mM $K_3Fe(CN)_6$, 0.5 mM $K_4Fe(CN)_6$, and 2 mM X-Gluc) at 37°C overnight (Tang et al., 2017). The stained tissues were then stored in decolorizing solution (70% ethanol and 30% ethanoic acid) for observation.

The DAB staining method was used for examination of H_2O_2 levels (Ben Rejeb et al., 2015). Three-week-old plants were syringe-infiltrated with *Pst* DC3000 (OD_{600} = 0.1), *Pst* DC3000 (AvrRps4; D_{600} = 0.1), or mock (10 mM $MgCl_2$) and sampled 24 h later. The inoculated leaves were transferred to the staining solution (1 mg mL^{-1} 3,3-Diaminobenzidine Sigma) for 12 h, and then decolorized in the destaining solution (70% ethanol and 30% ethanoic acid). For observation of dead cells, the inoculated leaves described above were transferred into a trypan blue solution (10 mL lactic acid, 10 mL glycerol, 10 g phenol, 10 mL H_2O, and 10 mg trypan blue) and boiled for 5 min (Koch and Slusarenko, 1990). The stained tissues were destained in a chloral hydrate solution overnight. The images were observed under a Leica M165C stereoscope.

Total RNA extraction and qRT-PCR analysis

For gene expression analysis in various tissues, the roots, stems, rosette leaves, flowers, and siliques were collected from Col plants. For gene expression analysis in response to

pathogens, 3-week-old plants were dip inoculated with *Pst* DC3000 (OD_{600} = 0.1), *Pst* DC3000 (AvrRps4; OD_{600} = 0.1), or mock (10 mM $MgCl_2$), and the leaves were collected at the indicated time points. All tissues were immediately placed in liquid nitrogen and stored at −80°C. Total RNA was extracted using the Plant RNA Kit (Promega Cat# LS1040). Quantitative RT-PCR was performed using a SYBR Green master mix (Vazyme, Cat# Q711-02) on a LightCycler 480 thermal cycler (Roche) as described previously (Liu et al., 2016). *ACTIN2* was used as an internal control for sample normalization in the real-time RT-PCR analysis ($2^{\Delta\Delta}C_t$ method). The primers used are listed in Supplemental Table 3.

Protein expression analysis

Three-week-old plants were dip inoculated with *Pst* DC3000 (OD_{600} = 0.1), *Pst* DC3000 (AvrRps4; OD_{600} = 0.1), or mock inoculated (10 mM $MgCl_2$). Total proteins, nuclei-depleted fractions, and nuclei-enriched fractions were extracted from infected leaves as previously described (Kinkema et al., 2000). Chloroplast components were separated by density gradient purification (Merendino et al., 2003). Proteins were subsequently resolved by sodium dodecyl sulfate-polyacrylamide gel electrophoresis (SDS–PAGE) and detected using anti-HA (Santa Cruz, Cat# sc-7392; 1:5,000 (v/v) dilution), anti-FLAG (Sigma, Cat# F3165; 1:10,000 (v/v) dilution), anti-actin (Novogene, Cat# NHT0049; 1:10,000 (v/v) dilution), anti-ribulose 1,5 bisphosphate carboxylase (RbcL; SAB, Cat# 44091; 1:10,000 (v/v) dilution), anti-H3 (Easybio, Cat# BE7004; 1:10,000 (v/v) dilution), and anti-phosphoenolpyruvate carboxylase (PEPC; Agrisera, Cat# AS09 458S; 1:2,000 (v/v) dilution) antibodies. Arabidopsis ACTIN, the large subunit of RbcL/oxygenase (Armbruster et al., 2014), PEPC (Liu et al., 2017), and histone H3 were used as total protein, chloroplastic, cytoplasmic, and nuclear markers, respectively. The relative intensity of protein bands was calculated using ImageJ software.

Yeast two-hybrid assay

Yeast two-hybrid assays were performed as described using the Yeastmaker Yeast Transformation System2 (Clontech). Full length or truncated versions of the coding regions of EDS1 and EIJ1 were amplified and cloned into *pGBKT7* (containing the DNA-binding domain, BD) or *pGADT7* (containing the GAL4 activation domain, AD) vectors (Clontech), respectively. The primers used are listed in Supplemental Table 3. Yeast AH109 cells were cotransformed with specific bait and prey constructs (Li et al., 2019). For yeast two-hybrid screening, BD-EDS1 was used as bait to screen an Arabidopsis cDNA library (CD4-30, from ABRC; Fan et al., 1997). All yeast transformants were grown on SD/-Trp/-Leu or SD/-Trp/-Leu/-His/-Ade mediums for screening or protein interaction test (Huang et al., 2015).

Pull-down assay

For prokaryotic protein expression, the coding regions of *EDS1* and *EIJ1* were cloned into the *pGEX-4T-1* (Pharmacia) and *pQE30* (QIAGEN) vectors to generate *GST-EDS1* and *His-EIJ1* constructs for expression in *Escherichia coli* Rosetta, respectively. Primers used are listed in Supplemental Table 3. For pull-down assays, His-EIJ1 was incubated with the GST or GST-EDS1 immobilized onto glutathione-sepharose beads (GE Healthcare, Cat# 17-0756-01) in binding buffer (50 mM Tris–HCl, pH 8.0, 100 mM NaCl, and 1 mM Ethylene Diamine Tetraacetie Acid (EDTA)) at 4°C overnight. After three washes with binding buffer, proteins retained on the beads were resolved by SDS–PAGE and detected using an anti-His antibody (BPI, Cat# AbM59012-18-PU; 1:5,000 (v/v) dilution) or an anti-GST antibody (BPI, Cat# AbM59001-2H5-PU; 1:10,000 (v/v) dilution). Pull-down assays were carried out as previously described (Zentella et al., 2017). The proteins extracted from *eij1-1* $35S_{pro}$*:EIJ1-6HA* transgenic plants were incubated with recombinant GST or GST-EDS1 immobilized onto glutathione-sepharose beads at 4°C overnight. Proteins retained on the beads were subsequently resolved by SDS-PAGE and detected using anti-HA, anti-GST antibody, anti-H3, and anti-PEPC as described above.

Co-IP assay

Leaves of 3-week-old $35S_{pro}$*:EIJ1-HA* $35S_{pro}$*:EDS1-FLAG* plants with or without *Pst* DC3000 treatment were harvested at 4 hpi. Total proteins, nuclei-depleted fractions, nuclei-enriched fractions, and chloroplast extracts were incubated with either an anti-FLAG agarose conjugate or agarose preimmune serum (IgG) in the Co-IP buffer (Hu et al., 2018) at 4°C overnight. After washed by Co-IP buffer three times, proteins retained on the beads were resolved by SDS–PAGE and detected by anti-FLAG or anti-HA antibody.

Phylogenetic analysis

Multiple alignments of amino acid sequences were performed using ClustalW2. The phylogenetic tree was constructed using the neighbor-joining method in MEGA software (version 5.2).

Cell-free protein degradation assay

Three-week-old *eds1-2* and Col plants were dip-inoculated with *Pst* DC3000 (OD_{600} = 0.1) for 12 h. Cell extracts were extracted in the degradation buffer (20 mM Tris–HCl pH 7.5, 100 mM NaCl, 10 mM $MgCl_2$, 5 mM DTT, and 10 mM ATP). The equal cell extracts (100 μL containing 500 μg total proteins) from different genotypes were incubated with equal His-EIJ1 recombinant protein at 30°C for time course degradation assays. Proteins were subsequently resolved by SDS–PAGE and detected using anti-His (BPI) and anti-actin antibodies, respectively (Novogene).

Transient expression assay

$PR1_{pro}$*:GUS* and $ICS1_{pro}$*:GUS* reporter constructs were generated as previously described (Li et al., 2019). The coding regions of *EIJ1*, *EIJ1* N-terminal, and *EDS1* were cloned into the *pGreen-35S-HA* or *pZPY122-35S-3FLAG* vector under the control of *35S* promoter and used as effectors. All primers used for these constructs are listed in Supplemental Table 3.

A construct containing firefly luciferase driven by 35S promoter was used as an internal control to evaluate transfection efficiency (Li et al., 2019). *Nicotiana benthamiana* leaves were infiltrated and cultured as previously described (Li et al., 2019). Relative GUS activity was calculated by normalizing against the luciferase activity, and the data presented were from three biological replicates.

RNA-Seq analysis

Three-week-old of *eij1-1*, *eds1-22*, and Col plants were dip inoculated with *Pst* DC3000 (OD_{600} = 0.1) or mock (10 mM $MgCl_2$). The treated leaves were collected at 24 hpi. Total RNA was extracted using the Plant RNA Kit (Promega), further purified using an RNeasy Mini Kit (Qiagen), and then subjected to quality control with an Agilent Bioanalyzer. The libraries were constructed using an Ultra RNA sample preparation kit (Illumina). Qubit2.0 and Agilent 2100 were used to detect the library concentration and insert size, respectively. The concentration of the library was further quantified using the Q-PCR method.

RNA sequencing was performed by the Biomarker Technologies Corporation (Beijing, China) using an Illumina NovaSeq platform, resulting in 23–33 million reads per sample. All the downstream analyses were based on clean data with high quality mapped to the Arabidopsis TAIR10 genome. Differential expression analysis of two conditions/groups was performed using the DESeq Ractiv package (1.18.0). The DEGs were identified by the program $Cuff_{diff}$ with the criteria set as q-value < 0.0001 and fold change > 2. Three valid biological replicates were carried out for the transcriptomic analysis. The gene expression patterns were graphically represented in a heat map by cluster analysis tool. GO analysis was performed using the GO annotation of The Arabidopsis Information Resource. Part of *eds1-22* data has been published in our recent study (Li et al., 2019).

Fluorescence microscopy

Fluorescence images were generated using a confocal laser-scanning microscope (Leica TCS SP5). 405 nm laser, 488 nm laser, and 587 nm laser were used to detect DAPI, GFP, and mCherry excitation, respectively. Images within a panel were taken using the same confocal settings.

Accession numbers

Sequencing data from this article can be found in the NCBI Gene Expression Omnibus database under accession number GSE140765. Accession numbers for proteins studied here are as follows: EIJ1 (AT2G24860), EDS1 (AT3G48090), ACTIN2 (AT3G18780), ICS1 (AT1G74710), PR1 (AT2G14610), and RbcL (ATCG00490). Germplasm used included *eij1-1* (SALK_142975), *eij1-2* (WiscDsLox343G09), and *eds1-22* (SALK_071051).

Supplemental data

Supplemental Figure 1. Amino acid sequence analysis of EIJ1.

Supplemental Figure 2. EIJ1 localizes to both the cytoplasm and nucleus.

Supplemental Figure 3. Expression analysis of *EIJ1-HA* in $35S_{pro}$:*EIJ1-HA*.

Supplemental Figure 4. Bacterial growth of *Pst* DC3000 on plants following pressure infiltration.

Supplemental Figure 5. Identification of the Arabidopsis *EIJ1* null allele *eij1-2*.

Supplemental Figure 6. *EDS1* is epistatic to *EIJ1*.

Supplemental Figure 7. Analysis of pathogen-responsive genes co-regulated by EIJ1 and EDS1.

Supplemental Figure 8. EDS1 causes the subcellular relocalization of EIJ1.

Supplemental Figure 9. EIJ1 regulates the nuclear vs. cytoplasmic distribution of EDS1.

Supplemental Figure 10. Transient analysis of *PR1* promoter activity regulated by EIJ1, N-EIJ1, and EDS1.

Supplemental Figure 11. Degradation of EIJ1 is independent of EDS1.

Supplemental Figure 12. EIJ1 retained on the chloroplast is unable to restore the disease resistance of *eij1-1*.

Supplemental Figure 13. Bacterial growth of Col and the *eij1-1* mutant.

Supplemental Figure 14. Loss of *EIJ1* function accelerates the nuclear translocation of EDS1 in infected plants.

Supplemental Figure 15. qRT-PCR analysis of *EIJ1* in response to pathogen infection.

Supplemental Table 1. GO categories of genes co-regulated by EIJ1 and EDS1.

Supplemental Table 2. Sources of plant materials.

Supplemental Table 3. Sequences of primers used in this study.

Supplemental references.

Supplemental Data Set 1. Statistical analysis data.

Supplemental Data Set 2. Genes regulated by EIJ1 and EDS1.

Supplemental File 1. Sequence alignment used to produce the phylogenetic tree in Supplemental Figure 1B.

Supplemental File 2. Replicate information.

Acknowledgments

We thank Dr. Haitao Cui for providing the *eds1-2* mutant.

Funding

This research was supported by grants from the "Strategic Priority Research Program" of the Chinese Academy of Sciences (grant no. XDA13020500), the National Natural Science Foundation of China (grant no. 32070289), and the Natural Science Foundation of Guangdong Province (grant no. 2017A030310654).

Conflict of interest statement. The authors declare that they have no conflict of interest.

References

Alvarez, ME, Pennell, RI, Meijer, PJ, Ishikawa, A, Dixon, RA, Lamb, C (1998) Reactive oxygen intermediates mediate a systemic signal network in the establishment of plant immunity. Cell **92**: 773–784

An, C, Mou, Z (2011) Salicylic acid and its function in plant immunity. J Integr Plant Biol **53**: 412–428

Armbruster, U, Carrillo, LR, Venema, K, Pavlovic, L, Schmidtmann, E, Kornfeld, A, Jahns, P, Berry, JA, Kramer, DM, Jonikas, MC (2014) Ion antiport accelerates photosynthetic acclimation in fluctuating light environments. Nat Commun **5**: 5439

Bartsch, M, Gobbato, E, Bednarek, P, Debey, S, Schultze, JL, Bautor, J, Parker, JE (2006) Salicylic acid-independent ENHANCED DISEASE SUSCEPTIBILITY1 signaling in Arabidopsis immunity and cell death is regulated by the monooxygenase FMO1 and the Nudix hydrolase NUDT7. Plant Cell **18**: 1038–1051

Ben Rejeb, K, Lefebvre-De Vos, D, Le Disquet, I, Leprince, AS, Bordenave, M, Maldiney, R, Jdey, A, Abdelly, C, Savouré, A (2015) Hydrogen peroxide produced by NADPH oxidases increases proline accumulation during salt or mannitol stress in Arabidopsis thaliana. New Phytol **208**: 1138–1148

Bukau, B, Weissman, J, Horwich, A (2006) Molecular chaperones and protein quality control. Cell **125**: 443–451

Caplan, J, Padmanabhan, M, Dinesh-Kumar, SP (2008) Plant NB-LRR immune receptors: from recognition to transcriptional reprogramming. Cell Host Microbe **3**: 126–135 10.1016/j.chom.2008.02.010

Dodds, PN, Rathjen, JP (2010) Plant immunity: towards an integrated view of plant-pathogen interactions. Nat Rev Genet **11**: 539–548

Dou, D, Zhou, J-M (2012) Phytopathogen effectors subverting host immunity: different foes, similar battleground. Cell Host Microbe **12**: 484–495

Du, Y, Zhao, J, Chen, T, Liu, Q, Zhang, H, Wang, Y, Hong, Y, Xiao, F, Zhang, L, Shen, Q (2013) Type I J-domain NbMIP1 proteins are required for both Tobacco mosaic virus infection and plant innate immunity. PLoS Pathog **9**: e1003659

Fan, H, Hu, Y, Tudor, M, Ma, H (1997) Specific interactions between the K domains of AG and AGLs, members of the MADS domain family of DNA binding proteins. Plant J **12**: 999–1010

Feys, BJ, Moisan, LJ, Newman, MA, Parker, JE (2001) Direct interaction between the Arabidopsis disease resistance signaling proteins, EDS1 and PAD4. EMBO J **20**: 5400–5411

García, AV, Blanvillain-Baufumé, S, Huibers, RP, Wiermer, M, Li, G, Gobbato, E, Rietz, S, Parker, JE (2010) Balanced nuclear and cytoplasmic activities of EDS1 are required for a complete plant innate immune response. PLoS Pathog **6**: e1000970

Gassmann, W, Hinsch, ME, Staskawicz, BJ (1999) The Arabidopsis RPS4 bacterial-resistance gene is a member of the TIR-NBS-LRR family of disease-resistance genes. Plant J **20**: 265–277

Gloggnitzer, J, Akimcheva, S, Srinivasan, A, Kusenda, B, Riehs, N, Stampfl, H, Bautor, J, Dekrout, B, Jonak, C, Jiménez-Gómez, JM (2014) Nonsense-mediated mRNA decay modulates immune receptor levels to regulate plant antibacterial defense. Cell Host Microbe **16**: 376–390

Ham, B-K, Park, JM, Lee, S-B, Kim, MJ, Lee, I-J, Kim, K-J, Kwon, CS, Paek, K-H (2006) Tobacco Tsip1, a DnaJ-type Zn finger protein, is recruited to and potentiates Tsi1-mediated transcriptional activation. Plant Cell **18**: 2005–2020

Heidrich, K, Blanvillain-Baufumé, S, Parker, JE (2012) Molecular and spatial constraints on NB-LRR receptor signaling. Curr Opin Plant Biol **15**: 385–391

Heidrich, K, Wirthmueller, L, Tasset, C, Pouzet, C, Deslandes, L, Parker, JE (2011) Arabidopsis EDS1 connects pathogen effector recognition to cell compartment–specific immune responses. Science **334**: 1401–1404

Hu, Y, Zhou, L, Huang, M, He, X, Yang, Y, Liu, X, Li, Y, Hou, X (2018) Gibberellins play an essential role in late embryogenesis of Arabidopsis. Nat Plants **4**: 289–298

Huang, M, Hu, Y, Liu, X, Li, Y, Hou, X. (2015) Arabidopsis LEAFY COTYLEDON1 mediates postembryonic development via interacting with PHYTOCHROME-INTERACTING FACTOR4. Plant Cell **27**: 3099–3111

Jelenska, J, Yao, N, Vinatzer, BA, Wright, CM, Brodsky, JL, Greenberg, JT (2007) A J domain virulence effector of Pseudomonas syringae remodels host chloroplasts and suppresses defenses. Curr Biol **17**: 499–508

Jones, J, Dangl, J (2006) The plant immune system. Nature **444**: 323–329

Khan, M, Subramaniam, R, Desveaux, D (2016) Of guards, decoys, baits and traps: pathogen perception in plants by type III effector sensors. Curr Opin Microbiol **29**: 49–55

Kinkema, M, Fan, W, Dong, X (2000) Nuclear localization of NPR1 is required for activation of PR gene expression. Plant Cell **12**: 2339–2350

Koch, E, Slusarenko, A (1990) Arabidopsis is susceptible to infection by a downy mildew fungus. Plant Cell **2**: 437–445

Lam, E, Kato, N, Lawton, M (2001) Programmed cell death, mitochondria and the plant hypersensitive response. Nature **411**: 848–853

Lee, DW, Kim, JK, Lee, S, Choi, S, Kim, S, Hwang, I (2008) Arabidopsis nuclear-encoded plastid transit peptides contain multiple sequence subgroups with distinctive chloroplast-targeting sequence motifs. Plant Cell **20**: 1603–1622

Li, Y, Yang, Y, Hu, Y, Liu, H, He, M, Yang, Z, Kong, F, Liu, X, Hou, X (2019) DELLA and EDS1 form a feedback regulatory module to fine-tune plant growth-defense tradeoff in Arabidopsis. Mol Plant **12**: 1485–1498

Liu, JZ, Whitham, SA (2013) Overexpression of a soybean nuclear localized type-III DnaJ domain-containing HSP40 reveals its roles in cell death and disease resistance. Plant J **74**: 110–121

Liu, X, Hu, P, Huang, M, Tang, Y, Li, Y, Li, L, Hou, X (2016) The NF-YC–RGL2 module integrates GA and ABA signalling to regulate seed germination in Arabidopsis. Nat Commu **7**: 1–14

Liu, Z, Jia, Y, Ding, Y, Shi, Y, Li, Z, Guo, Y, Gong, Z, Yang, S (2017) Plasma membrane CRPK1-mediated phosphorylation of 14-3-3 proteins induces their nuclear import to fine-tune CBF signaling during cold response. Mol Cell **66**: 117–128

Loake, G, Grant, M (2007) Salicylic acid in plant defence-the players and protagonists. Curr. Opin Plant Biol **10**: 466–472

Melotto, M, Underwood, W, Koczan, J, Nomura, K, He, SY (2006) Plant stomata function in innate immunity against bacterial invasion. Cell **126**: 969–980

Merendino, L, Falciatore, A, Rochaix, JD (2003) Expression and RNA binding properties of the chloroplast ribosomal protein S1 from Chlamydomonas reinhardtii. Plant Mol Biol **53**: 371–382

Nanda, AK, Andrio, E, Marino, D, Pauly, N, Dunand, C (2010) Reactive oxygen species during plant-microorganism early interactions. J. Integr Plant Biol **52**: 195–204

Park, JM, Park, CJ, Lee, SB, Ham, BK, Shin, R, Paek, KH (2001) Overexpression of the tobacco Tsi1 gene encoding an EREBP/AP2-type transcription factor enhances resistance against pathogen attack and osmotic stress in tobacco. Plant Cell **13**: 1035–1046

Parker, JE, Holub, EB, Frost, LN, Falk, A, Gunn, ND, Daniels, MJ (1996) Characterization of eds1, a mutation in Arabidopsis suppressing resistance to Peronospora parasitica specified by several different RPP genes. Plant Cell **8**: 2033–2046

Pulido, P, Leister, D (2018) Novel DNAJ-related proteins in Arabidopsis thaliana. New Phytol **217**: 480–490

Rietz, S, Stamm, A, Malonek, S, Wagner, S, Becker, D, Medina-Escobar, N, Corina Vlot, A, Feys, BJ, Niefind, K, Parker, JE (2011) Different roles of Enhanced Disease Susceptibility1 (EDS1) bound to and dissociated from Phytoalexin Deficient4 (PAD4) in Arabidopsis immunity. New Phytol **191**: 107–119

Rustérucci, C, Aviv, DH, Holt, BF, Dangl, JL, Parker, JE (2001) The disease resistance signaling components EDS1 and PAD4 are

essential regulators of the cell death pathway controlled by LSD1 in Arabidopsis. Plant Cell **13**: 2211–2224

Saikat, B, Halane, MK, Hee, KS, Walter, G (2011) Pathogen effectors target Arabidopsis EDS1 and alter its interactions with immune regulators. Science **334**: 1405–1408

Serrano, M, Wang, B, Aryal, B, Garcion, C, Abou-Mansour, E, Heck, S, Geisler, M, Mauch, F, Nawrath, C, Metraux, JP (2013) Export of salicylic acid from the chloroplast requires the multidrug and toxin extrusion-like transporter EDS5. Plant Physiol **162**: 1815–1821

Tang, Y, Liu, X, Liu, X, Li, Y, Wu, K, Hou, X (2017) Arabidopsis NF-YCs mediate the light-controlled hypocotyl elongation via modulating histone acetylation. Mol Plant **10**: 260–273

Torres, MA, Jones, JD, Dangl, JL (2006) Reactive oxygen species signaling in response to pathogens. Plant Physiol **141**: 373–378

Tsuda, K, Katagiri, F (2010) Comparing signaling mechanisms engaged in pattern-triggered and effector-triggered immunity. Curr Opin Plant Biol **13**: 459–465

Wagner, S, Stuttmann, J, Rietz, S, Guerois, R, Brunstein, E, Bautor, J, Niefind, K, Parker, JE (2013) Structural basis for signaling by exclusive EDS1 heteromeric complexes with SAG101 or PAD4 in plant innate immunity. Cell Host Microbe **14**: 619–630

Wang, G, Cai, G, Kong, F, Deng, Y, Ma, N, Meng, Q (2014) Overexpression of tomato chloroplast-targeted DnaJ protein enhances tolerance to drought stress and resistance to Pseudomonas solanacearum in transgenic tobacco. Plant Physiol Bioch **82**: 95–104

Wiermer, M, Feys, BJ, Parker, JE (2005) Plant immunity: the EDS1 regulatory node. Curr Opin Plant Biol **8**: 383–389

Wirthmueller, L, Zhang, Y, Jones, JD, Parker, JE (2007) Nuclear accumulation of the Arabidopsis immune receptor RPS4 is necessary for triggering EDS1-dependent defense. Curr Biol **17**: 2023–2029

Xin, X-F, He, SY (2013) Pseudomonas syringae pv. tomato DC3000: a model pathogen for probing disease susceptibility and hormone signaling in plants. Annu Rev Phytopathol **51**: 473–498

Yang, L, Li, B, Zheng, XY, Li, J, Yang, M, Dong, X, He, G, An, C, Deng, XW (2015) Salicylic acid biosynthesis is enhanced and contributes to increased biotrophic pathogen resistance in Arabidopsis hybrids. Nat Commun **6**: 7309

Yang, S, Hua, J (2004) A haplotype-specific Resistance gene regulated by BONZAI1 mediates temperature-dependent growth control in Arabidopsis. Plant Cell **16**: 1060–1071

Zentella, R, Sui, N, Barnhill, B, Hsieh, W-P, Hu, J, Shabanowitz, J, Boyce, M, Olszewski, NE, Zhou, P, Hunt, DF et al. (2017) The Arabidopsis O-fucosyltransferase SPINDLY activates nuclear growth repressor DELLA. Nat Chem Biol **13**: 479

Zhong, X, Yang, J, Shi, Y, Wang, X, Wang, GL (2018) The DnaJ protein OsDjA6 negatively regulates rice innate immunity to the blast fungus Magnaporthe oryzae. Mol Plant Pathol **19**: 607–614

Zipfel, C (2008) Pattern-recognition receptors in plant innate immunity. Curr Opin Immunol **20**: 10–16